New insights into the provenance of Saudi Arabian Palaeozoic sandstones from heavy mineral analysis and single-grain geochemistry

Alexander Bassis[a,*], Matthias Hinderer[a], Guido Meinhold[b]

[a]Institute of Applied Geosciences, Darmstadt Technical University, Schnittspahnstraße 9, 64287 Darmstadt, Germany

[b]Department of Sedimentology & Environmental Geology, Geoscience Centre, University of Göttingen, Goldschmidtstraße 3, 37077 Göttingen, Germany

* Corresponding author. Tel. +49 6151 1675552; fax: +49 6151 166539.

E-mail address: bassis@geo.tu-darmstadt.de (A. Bassis).

Abstract

Saudi Arabian Palaeozoic siliciclastics cover a stratigraphic range from the Cambrian to the Permian. They crop out along the eastern margin of the Arabian Shield and are comprised of highly mature sandstones. Their heavy mineral assemblage reflects their mineralogical maturity and is dominated by the ultra-stable phases zircon, tourmaline and rutile. Less stable accessories are apatite, staurolite and garnet. Standard heavy mineral analysis of samples from two study areas in central/northern (Tabuk area) and southern (Wajid area) Saudi Arabia reveals distinct changes in provenance. Cambrian–Ordovician sandstones are first-cycle sediments, probably sourced from the 'Pan-African' basement. The overlying Hirnantian glaciogenic deposits consist of recycled Cambrian–Ordovician material.

Devonian–Permian sandstones show a significant influx of fresh basement material, as attested by an increase of meta-stable heavy minerals. Single-grain geochemical analysis of rutile and garnet has proven to be a powerful supplementary technique. Rutile varietal studies reveal distinct differences in host rock lithologies between the two study areas: the Tabuk area contains predominantly felsic rutiles, whereas the Wajid area has more mafic input. Zr-in-rutile thermometry identified granulite-facies detritus in the lower Palaeozoic of the Tabuk area and has the potential to further define source areas. The distribution patterns of garnet host rock lithologies are remarkably similar in both study areas. They are dominated by amphibolite-facies metasediments and intermediate to felsic igneous rocks. Garnets derived from granulite-facies metasediments, which are scarce in the Arabian–Nubian Shield, also occur. Possible source rocks for high-grade garnets can be found in Yemen or farther south in the Mozambique Belt.

Keywords: Saudi Arabia; Palaeozoic; provenance; heavy minerals; quartz arenite

1. Introduction

The Palaeozoic succession of Saudi Arabia is dominated by highly mature siliciclastics. Sandstones crop out in a narrow band that extends over 1500 km NW–SE along the southern, eastern and northern margin of the Arabian Shield (Fig. 1a). The succession reaches a thickness of about 500 m in the outcrop and dips slightly eastwards. It continues in the subsurface, where it can reach a thickness of up to 4500 m and contains important hydrocarbon source and reservoir rocks (McGillivray and Husseini, 1992; Al-Ajmi et al., 2015). Deposition took place from the Cambrian to the Permian (Fig. 2**Error! Reference source not found.**), but age control has proven to be difficult in the mostly fossil-barren units. Depositional environments are varied, ranging from fluvial braided stream conditions to shallow marine, prodeltaic and open marine settings (Al-Ajmi et al., 2015). Several erosional hiatuses separate the sedimentary units and are used for lithostratigraphic correlations.

Prominent are glaciogenic and proglacial sediments and features associated with the Hirnantian as well as Carboniferous–Permian Gondwana glaciations. According to the common and widely accepted model, the Palaeozoic succession was deposited on a stable continental shelf at a passive margin, leading to the development of a 'layer cake' stratigraphy (Sharland et al., 2001). The exact source for the Palaeozoic detritus is still under debate. The adjacent Arabian Shield most likely was a major contributor throughout the Palaeozoic, but far distant sources have to be taken into account as well (Al-Harbi and Khan, 2005, 2008, 2011; Wanas and Abdel-Maguid, 2006). Possible source areas to the south include Archean to Palaeoproterozoic terranes in Yemen (Babalola, 1999; Hussain et al., 2000, 2004; Hussain, 2001), metamorphic terranes in Eritrea and Sudan, as well as the Mozambique Belt in East Africa. A significant recycled sedimentary source is a possibility that so far could neither be proven nor refuted.

The high maturity of Palaeozoic sandstones coupled with the poor fossil record create unique problems for the interpretation of sedimentary provenance and stratigraphic correlation. Lithostratigraphic correlations in the very uniform successions are unreliable and imprecise, especially in the subsurface. Bulk-rock geochemistry can help with correlations and to infer tectonic setting and provenance, but is also dependant on modal composition. The method therefore also suffers from the poor diversity of mature siliciclastics. Another way to tackle the problem is the study of the heavy mineral fraction. Standard heavy mineral analysis (SHMA, modal analysis) has been an important tool in provenance studies, both in ancient and recent sediments (Mange and Wright, 2007). So far, several workers have applied SHMA to the Palaeozoic succession, but have mostly concentrated their efforts on the Wajid outcrop belt of southern Saudi Arabia (Babalola, 1999; Hussain et al., 2000, 2004; Hussain, 2001; Hussain and Abdullatif, 2004; Knox et al., 2007). These studies noted the dominance of the ultra-stable fraction of zircon, tourmaline and rutile in the heavy mineral assemblage. Hussain (2001) interpreted this as the result of intensive weathering, whereas for Hussain et al. (2004) it is a clear indicator for sedimentary recycling. Babalola (1999), Hussain (2001), Hussain and

Abdullatif (2004) and Hussain et al. (2004) identified acidic to intermediate igneous rocks in Yemen as the most likely source for the Wajid Group. According to these studies, other sources like metamorphic, mafic igneous and sedimentary rocks as well as the Arabian Shield to the west are only minor contributors. Knox et al. (2007) identified several distinct heavy mineral zones and significant changes in provenance signatures throughout the Wajid Group. Only a few studies have targeted the central and northern part of the country, with varying success (Powers et al., 1966; Hussain and Abdullatif, 2004; Knox et al., 2010). Powers et al. (1966) conducted a pilot study to assess the potential of heavy mineral analysis. They report a dominant ultra-stable fraction from the Saq and overlying formations (Fig. 2), which they interpreted as indicative for sedimentary recycling. Yet they also found mica (biotite and muscovite), which is surprising given its unstable nature during transport. Hussain and Abdullatif (2004) also report an abundance of the zircon, tourmaline and rutile from the Saq and Qasim formations (Fig. 2), but were unable to use their heavy mineral data for correlations. Knox et al. (2010) on the other hand were successful in studying heavy mineral assemblages of the Unayzah Formation (Fig. 2) from wells. They identified two changes in provenance within the Unayzah Formation, dividing it into three different heavy mineral units. They also tentatively recognise the potential of heavy mineral analysis for regional correlations.

In recent years, several studies were published dealing with provenance and heavy mineral studies on the northern margin of Gondwana. Most of them feature U–Pb age dating of detrital zircons, but also touch upon SHMA. Avigad et al. (2003, 2005) and Kolodner et al. (2006) used SHMA and U–Pb dating of detrital zircons from Cambrian–Ordovician sandstones from southern Israel to deduce provenance and palaeoclimate. Morag et al. (2011) utilized the corresponding Hf isotopic data to infer long-distance transport for Cambrian–Ordovician sediments. Weissbrod and Bogoch (2007) compiled heavy mineral data of Neoproterozoic to Mesozoic siliciclastic sediments from the northern margin of the Arabian–Nubian Shield (ANS) and provide a comprehensive review of heavy mineral studies in that area. Morton et al. (2011) and Meinhold et al. (2011, 2013) studied heavy mineral assemblages and detrital zircon ages of Precambrian to Mesozoic siliciclastic sediments from the Murzuq basin, Libya, in order to reconstruct provenance, palaeogeography and stratigraphic correlations. Linnemann et al. (2011) conducted a provenance analysis employing detrital zircon U–Pb geochronology of Cambrian–Ordovician sandstones from the Algerian Sahara. They identified a range of several different cratons and terranes as sources areas, but excluded the ANS as a potential source. In their study concerning the provenance of recent Arabian desert sand, Garzanti et al. (2013) also analysed the heavy mineral assemblages and detrital zircon ages of two samples from the lower Palaeozoic of northern Saudi Arabia.

While the sandstones from the Wajid area have been studied by several workers, data from the central and northern Saudi Arabian succession is still scarce. With this study we intend to link and compare the Wajid outcrop belt with the Palaeozoic successions in central and northern Saudi Arabia. We also mean to reveal changes in sedimentary provenance in time by studying representative samples throughout the northern/central and southern successions, covering the entire Palaeozoic. A further goal is to link Saudi Arabian sandstones with other parts of the northern Gondwana margin, utilising both SHMA and single-grain techniques.

1.1 Study area and stratigraphic framework

The study area is located along the southern and eastern margin of the Arabian Shield as well as to the north around the city of Sakaka (Fig. 1). Outcrops of the northern study area (‘Tabuk area’) (Fig. 1c) are found mainly around the cities of Buraida, Hail and Sakaka. The early Palaeozoic is dominated by fluvial and shallow marine deposits of the Middle Cambrian to Late Ordovician Saq and Qasim formations (Powers et al., 1966; Sharland et al., 2001; Hussain and Abdullatif, 2004; Hussain, 2007). The Saq Formation consists of poorly- to well-sorted, cross-bedded, mature sandstone. In contrast, the Qasim Formation consists of cyclic alternations of thin bedded, fine-grained sandstone to shale and thick-bedded, massive to cross-bedded sandstone. Both formations are deeply eroded by glacial tunnel valleys of the Hirnantian Sarah and Zarqa formations (Senalp and Al-Laboun, 2000), which are treated as one unit in this study. The tunnel valley fill consists of glacial tillites, micaceous and sometimes cross-bedded sandstones. The Sarah and Zarqa formations are unconformably overlain by the Middle Silurian, predominantly shaly Sharawra Member of the Qalibah Formation (Senalp and Al-Laboun, 2000; Melvin, 2015). Another hiatus separates the Silurian shales from the fluvial to shallow marine Devonian units of the Tawil, Jauf and Jubah formations. The Tawil and Jubah formations consist of fine-grained siltstones and shales alternating with fine- to medium-grained sandstones, whereas the Jauf Formation is predominantly shaly with intercalations of limestone, dolomite and fine-grained sandstone. After another stratigraphic gap spanning most of the Carboniferous follows the Unayzah Formation. It comprises various conglomerates, fine- to coarse-grained sandstones with intercalated siltstones and shales. They were deposited during the Late Carboniferous to Middle Permian in a glaciofluvial to glaciolacustrine environment (Alsharhan, 1994; Sharland et al., 2001).

In the southern study area (‘Wajid area’, Fig. 1b), Palaeozoic sandstones from the Cambrian through the Permian are spectacularly exposed south of the town of Wadi Ad Dawasir. The Wajid Group, comprising of the Dibsiyah, Sanamah, Khusayyayn and Juwayl formations as well as the Qusaiba Member of the Qalibah Formation (Fig. 2) has been comprehensively studied in the past (Al-Ajmi et al., 2015, and references therein). The late Cambrian to early Ordovician Dibsiyah Formation consists of highly mature, medium- to coarse-grained sandstones. It was deposited under shallow marine conditions and contains spectacular *Skolithos* ichnofacies (Al-Ajmi et al., 2015). Subglacial tunnel valleys of the Hirnantian Sanamah Formation unconformably overlie and deeply erode into the Dibsiyah Formation (Al-Ajmi et al., 2015). The tunnel valleys are NW–SE trending and are filled with various conglomerates, medium- to coarse-grained sandstones, siltstones and shales (Keller et al., 2011). Following are the shales of the Silurian Qusaiba Member of the Qalibah Formation. It was deposited in a low-energy open marine setting (Lüning et al., 2000). The overlying Sharawra Member is absent in the Wajid area. A hiatus separates the Qusaiba Member from the early Devonian Khusayyayn Formation, which consists of medium- to coarse-grained, partly conglomeratic sandstones with large-scale cross-bedding. Deposition of the rather uniform succession took place under shallow marine conditions (Al-Ajmi et al., 2015). The next preserved unit is the late Carboniferous to early Permian Juwayl Formation. It consists of matrix-supported conglomerates, medium- to coarse-grained, massive to cross- and ripple-bedded sandstones, siltstones and shales. Deposition took place in two principal, distinctly glaciofluvial environments (Keller et al., 2011).

1.2 Heavy Minerals

Heavy mineral assemblages can be indicative for source rock lithology. Processes during transport, deposition and burial leave the relative abundances of heavy minerals largely unaffected, provided they share a similar hydraulic and diagenetic behaviour (Morton and Hallsworth, 1999). However, intensive weathering, reworking or sedimentary recycling may severely reduce the variability within the heavy mineral assemblages of mature sandstones. In such a case, the examination of the variability – for example crystal structure, internal layout or chemical composition – of single grains from the same mineral phase (‘varietal studies’) is an ideal complementary technique. Geochemical varietal studies are frequently conducted using a wide array of heavy minerals: garnet, Cr-spinel, tourmaline, pyroxenes, amphiboles, apatite as well as chloritoid, epidote, rutile and monazite, among others (Mange and Morton, 2007). To successfully conduct varietal studies the samples have to contain statistically significant amounts of the respective mineral. This is a fundamental challenge when studying highly mature siliciclastics with impoverished heavy mineral assemblages. A lot of the meta- and unstable phases are not preserved in sufficient numbers. The consequence is to target the ultra-stable fraction and/or any meta-stable or labile phase that occurs in acceptable quantity. For this and other reasons, rutile and garnet were selected for single-grain geochemical analysis in this study. They both have variable chemical compositions, especially garnet, and their composition is provenance-dependant (Morton et al., 2004; Mange and Morton, 2007; Zack et al., 2004a; Meinhold et al., 2008; Meinhold, 2010; Triebold et al., 2012; Krippner et al., 2014). Furthermore rutile is part of the ultra-stable fraction and is present in sufficient abundance throughout the successions of both study areas. Garnet, although not as resistant and stable as rutile, occurs in late Palaeozoic formations. Additionally the chemical composition of both can be measured in a non-destructive way utilising an electron-microprobe (EMP).

1.2.1 Heavy mineral indices

Although a reliable provenance indicator under the right circumstances, the composition of heavy mineral assemblages from the same source rock can be altered and modified by many processes. Among those are: destruction of unstable grains by chemical weathering, hydraulic sorting during transport, sorting by grain size and diagenetic alteration (Morton and Hallsworth, 1999; Garzanti et al., 2008, 2009). These processes can affect a detrital heavy mineral assemblage in such a way that it no longer resembles the one from its source rock (Knox et al., 2007). Therefore results obtained by only studying percentage data can be unreliable. A remedy for this issue is the study of indices from heavy minerals of the same grain size that have similar hydraulic properties and are resistant to diagenetic alteration and weathering (Morton, 1985; Morton and Hallsworth, 1994, 1999; Knox et al., 2007). Indices used in this study include the zircon–tourmaline–rutile index (ZTR) (Hubert, 1962), the rutile–zircon index (RZi), the garnet–zircon index (GZi), the apatite–tourmaline index (ATi) and the staurolite–tourmaline index (STi) (Morton and Hallsworth, 1994, 1999) (Table 1). The heavy mineral indices are discussed in detail in Morton and Hallsworth (1994, 1999) and Knox et al. (2007).

1.2.2 Rutile

Rutile is formed predominantly in medium- to high-grade metamorphic rocks, which are regarded as the primary source for detrital rutile. It also can be found in low-grade metamorphic rocks, quartz veins and in different igneous rocks (Meinhold, 2010). This variability coupled with its high chemical and physical stability make rutile a prime candidate for provenance studies (e.g., Meinhold et al., 2008; Meinhold, 2010; Triebold et al., 2012).

The concept of source lithology characterisation in 'mafic' and 'felsic', utilising the Cr–Nb system of rutile, has first been proposed by Zack et al. (2004a) and then further refined by Triebold et al. (2007), Meinhold et al. (2008) and most recently by Triebold et al. (2012) with the following criteria:

$$x = 5 * (Nb_{ppm} - 500) - Cr_{ppm} \qquad (1)$$

where mafic rutiles have x < 0 and felsic rutiles have a x > 0.

The dependency of the Zr content of rutiles on pressure and temperature can be used for Zr-in-rutile thermometry (Zack et al., 2004b; Watson et al., 2006; Tomkins et al., 2007). For this study, the Zr-in-rutile thermometer after Tomkins et al. (2007) has been used:

$$T\,[°C] = \frac{83.9 + 0.14 * P}{0.1428 - R * \ln(Zr_{ppm})} - 273 \qquad (2)$$

with P = 10 kbar (as suggested by Triebold et al., 2012, for cases with unknown growth pressure) and the gas constant R = 0.0083144 kJ/K. It gives similar results at 10 kbar like the thermometer of Watson et al. (2006). The maximum divergence of 8 K between both thermometers is well within their margins of error (± 20 °C).

1.2.3 Garnet

The varied chemical composition of garnet, which is dependent on host rock lithology, and its occurrence in a wide range of metamorphic as well as igneous rocks, coupled with a relatively high stability make it suitable for provenance analysis (Krippner et al., 2014). Consequently, garnet has been utilised in provenance studies of sediments ranging from the Palaeozoic to the Holocene (Mange and Morton, 2007, and references therein).

2. Methodology

A total of 40 samples of ~2–3 kg each has been collected from two study areas. In both areas representative units covering the entire Palaeozoic succession were sampled. Sample locations are shown in Fig. 1; GPS coordinates and inferred stratigraphic order are given in the accompanying Supplementary data (see Appendix A). During sampling, emphasize has been put on fine- to medium-grained sandstones. This grain size range is representative for most formations and usually provides good heavy mineral yields. Preparation of samples was mostly done at Darmstadt Technical University. The rocks were first cut with a standard rock saw and then crushed by a jaw crusher. To disintegrate the grain framework without damaging the heavy minerals, the material was ground by a vibratory disc mill with a tungsten carbide set for 30 seconds. The 63–125 µm fraction was separated by dry sieving. Heavy minerals have been extracted in separation funnels by density separation with sodium polytungstate ($Na_6[H_2W_{12}O_{40}]$) with a density of 2.855 g/cm^3.

2.1 Standard heavy mineral analysis

The heavy minerals were mounted on a thin section slide with Epo-Tek 301 two-component resin and covered with a glass plate. SHMA was performed by counting under a petrographic microscope. First the ratio of translucent to opaque grains was determined by counting 200 grains per sample. In a second run, 300 translucent grains were counted to determine the abundance of translucent detrital heavy minerals. Where not enough translucent heavy minerals were available, all grains were counted. Mineral identification was done with the help of Mange and Maurer (1992).
Results of SHMA have been plotted in their inferred stratigraphic order in Fig. 3 and Fig. 5. Note that there is some degree of uncertainty about the exact order of the samples. Due to the lack of stratigraphic markers, the distances

between outcrops and the sedimentary architecture of some units, precise stratigraphic positioning of the samples was not always possible.

2.2 Varietal studies

From the lower and upper Palaeozoic successions of each study area, seven samples (three from the Tabuk area, four from the Wajid area) were randomly chosen for rutile varietal studies. Samples for garnet geochemical analysis were chosen regarding high abundance. Rutiles and garnets were hand-picked from the heavy mineral residuum under a binocular and placed on synthetic mounts. Single-grain geochemical analyses of rutile and garnet were performed with a JEOL JXA 8900 RL EMP equipped with five wavelength dispersive spectrometers at the Geoscience Center at the University of Göttingen. Measuring conditions for rutile include a beam current of 80 nA and an accelerating voltage of 25 kV. The counting times per spot were 200 s for Nb, Al, Cr, Zr and V, 100 s for Sn, Si, Fe and W, and 15 s for Ti. Measuring conditions for garnet include a beam current of 20 nA and an accelerating voltage of 15 kV. The counting times per spot were 15 s for Si, Mg, Ca, Fe, and Al, and 30 s for Ti, Cr, and Mn. Detection limits and standard errors are given together with the analytical data in the accompanying Supplementary Data (see Appendix A).

3. Results

3.1 Standard heavy mineral analysis

Results of SHMA are shown in Figs. 3 and 5 and Tables 2 and 3. They are presented as averages for each formation. The ratio of opaque phases to translucent heavy minerals is high on average (between 58% and 97%). The heavy mineral suites of the Palaeozoic successions from both study areas are dominated by the ultra-stable set of zircon, tourmaline and rutile. Among the ultra-stables, zircon is the most abundant phase in most samples, followed by tourmaline, while rutile is the least abundant of the three. Most of the encountered zircons were rounded (Fig. 4a). Some euhedral zircons were observed, but they seemed to be evenly distributed throughout all formations (Fig. 4b). Zircons were mostly colourless with only very few having a slight yellowish tint. Tourmaline was encountered as both rounded and prismatic grains (Fig. 4d). Rutile grains were all rounded, no prismatic grains were found (Fig. 4c).

Apatite is roughly equally distributed among all formations, never amounting to more than 8% average translucent grains, with the exception of two samples from the Wajid area. Apatite, when encountered, was always well rounded (Fig. 4e, upper row).

Garnet occurs in significant amounts only in middle to late Palaeozoic samples from the Tabuk area. Garnet is less abundant in the Wajid area with the exception of one sample (AB-SA98), where garnet was the dominant phase. Garnets appeared weathered, but still angular. No prismatic grains were observed (Fig. 4f).

Staurolite appears mostly in the Juwayl and Khusayyayn formations of the upper Wajid area. Staurolite is almost absent in samples of the Tabuk area. Grains appear weathered but still sharply angular (Fig. 4e, lower row).

Other heavy minerals found in very small quantities encompass: monazite, kyanite, enstatite, epidote, tremolite, Cr-spinel, sphene and hornblende. They are rare and their combined share never exceeds 6.3% at the most, with the majority of samples containing between 0% and 3%.

The last encountered group of heavy minerals are altered grains. This class contains all translucent heavy minerals that are altered through overgrowths or diagenetic effects to the point where they could no longer be identified.

The results of the different heavy mineral indices used in this study are shown in Table 3 and have been plotted in their inferred stratigraphical order in Fig. 5.

3.1.1 Zircon–tourmaline–rutile index (ZTR)

The Cambrian–Ordovician sandstones of the Dibsiyah and Sanamah formations are distinguished by very high ZTR values, between 91% and 99%. These drop off markedly in younger units. Two drastic drops in ZTR content can be observed in the Qusaiba Member and Juwayl Formation of the Wajid area. Whereas the very low value of the Silurian Qusaiba Member is due to high amounts of altered grains, the uppermost sample from the Juwayl Formation is dominated by garnet. The distributional pattern is similar in the Tabuk area: very high ZTR content in the Cambrian–Ordovician units (between 90% and 100%) and slightly less in later Palaeozoic formations. The difference though is not as prominent as in Wajid area. Another similarity is the very low ZTR value of the Silurian Sharawra Member. As with the Qusaiba Member, this is due to high amounts of altered grains. It is worth noting however that the second sample from the Sharawra Member has a very high ZTR value of 94%.

3.1.2 Rutile–zircon index (RZi)

The RZi shows no immediately recognisable trend throughout the stratigraphic successions of both study areas. It stays mainly in the range of <10 to 20 in the Wajid area, with two noticeable increases in the Khusayyayn and Juwayl formations. These are treated as outliers, as the other samples from those formations show a RZi similar to the remainder of southern Saudi Arabian samples. In the Tabuk area the RZi is overall a little higher, mostly between 10 and >20. Samples from the Qasim Formation have slightly elevated RZi values compared to the remainder of the Tabuk area.

3.1.3 Garnet–zircon index (GZi)

The GZi is very low in most of the Wajid Group. Only a dozen grains have been encountered throughout the succession. While the sample from the Qusaiba Member has a comparatively high GZi in regards to the rest of the Wajid samples, this is due to the very low zircon amount and not an increased garnet content. The youngest sample from the Juwayl Formation (AB-SA98) is a striking exception; 163 garnets were counted, resulting in a GZi of 91. In the Tabuk area a clear trend can be seen in the GZi: Lower Palaeozoic samples have a very low garnet and consequently low GZi. Upper Palaeozoic samples on the other hand have a significant garnet component, resulting in GZi values of 5.8 to 37.

3.1.4 Apatite-tourmaline index (ATi)

The ATi in the Wajid area is generally below 20 but shows two distinct peaks. One centred on the Silurian Qusaiba Member, which has an ATi of 67.1. The second is found in the youngest Juwayl sample, which has an even higher ATi of 70. The Tabuk area does not display these spikes. Instead, there is a clear distinction between the Saq and Qasim formations and the remainder of the succession. While the former have a very low ATi or no apatite at all, the overlying units show values mostly between ~5 and ~20.

3.1.5 Staurolite–tourmaline index (STi)

The succession of the Wajid area has a recognisable trend, increasing from very low values in the Cambrian–Ordovician and Silurian units up to almost 60 in the top sample from the Permian Juwayl formation. A marked increase of the STi appears between the Silurian Qusaiba Member and the Devonian Khusayyayn Formation. Samples from the Tabuk area do not exhibit this trend and have overall low staurolite content, with the exception of the single sample from the Permian Unayzah Formation.

3.1.6 Opaque phases

The percentage of opaque phases versus translucent heavy minerals has also been plotted (Fig. 5). No clear trends were observed in both study areas, but there appears to be a minor distribution pattern in the Wajid succession. The mean opaque mineral content of the Dibsiyah, Sanamah and Juwayl formations is between 58% (Sanamah Formation) and 66% (Dibsiyah Formation). The Khusayyayn Formation and Qusaiba Member on the other hand have higher concentrations of 84% and 96%, respectively. The distribution of opaque heavy minerals in the Tabuk area is entirely erratic, with concentrations fluctuating between 25% and 98%.

3.1.7 Cross-plots

Heavy mineral indices have been cross-plotted after Knox et al. (2007). The RZi has been chosen as the common reference index, as it is the most indicative index for changes in provenance and because sufficient counts of both zircon and rutile were obtained from all samples. However, these cross-plots did not yield informative results. No separation of stratigraphic units or trends could be observed, except for single outlier samples. The plots are therefore not presented in this paper, but can be accessed as supplementary data.

3.2 Single-grain analysis

The mineral chemical data for rutile and garnet are provided as Supplementary Data (see Appendix A).

3.2.1 Rutile geochemistry

Results for rutile source rock classification are shown in Table 4 and in Fig. 6a and b. A total of 199 rutiles was measured from the upper and lower Palaeozoic successions of the Tabuk and Wajid areas. In the Tabuk area, rutiles from felsic source lithologies are dominant (Fig 6a). In the Wajid area, mafic rutiles were more abundant than in the Tabuk area (Fig. 6b). Results for the Zr-in-rutile thermometry are shown as frequency histograms of in Fig. 6. Each rutile has been assigned to a temperature population, with each population covering 50 °C. From the Wajid Group a total of 72 rutiles yielded usable Zr concentrations (i.e., above detection limit of EMP). Sandstones from the Tabuk area yielded a total of 123 suitable rutiles. Distributions of temperature populations from both study areas are similar. Most rutiles (71.6%) fall into the 600 °C to 700 °C range. A minor population (20.1%) displays temperatures below 550 °C, while only a few (8.3%) show temperatures higher than 750 °C. Very high-grade (granulite-facies) rutiles were only encountered in the Saq Formation (Fig. 6c).

3.2.2 Garnet geochemistry

Results of the garnet single-grain geochemical analysis are shown in the classification scheme after Mange and Morton (2007) (Fig. 7a). Some garnets were measured at the core and rim. Plot points for rim measurements are shown as black symbols in Fig. 7a and were not considered in further analyses. Garnet type distribution for the three studied formations is displayed as pie charts in Fig. 7b–d. Six measured garnets from the Jauf Formation mostly originate from high-grade metabasic rocks. From the Jubah Formation 50 garnets were measured in 3 samples. Amphibolite-facies type B garnets are dominant (78%). The Juwayl Formation has a similar distribution like the Jubah Formation with dominant amphibolite-facies garnets, but a larger portion of high-grade metabasic rocks. No type D garnets from Ca-rich metamorphic rocks were found in any of the samples.

4. Discussion

4.1 Standard heavy mineral analysis

The heavy mineral assemblages of the studied samples are typical for highly mature sandstones (Morton and Hallsworth, 1999; Mange and Wright, 2007). Dominant fractions are the ultra-stable minerals zircon, tourmaline and rutile, which are heavily resistant to weathering and diagenesis. Less stable heavy minerals, like apatite, staurolite and garnet make up only a fraction of the total assemblage, while metastable and unstable minerals are almost completely absent (Fig. 3). This distribution can be the result of several processes: a primary source signal from acidic igneous rocks, recycling of older sedimentary rocks, heavy weathering in the source area, reworking during deposition, dissolution after burial or any combination of those, through removal of less stable phases. The abundance of ultra-stable minerals alone gives no evidence which process was responsible and is in itself not a reliable provenance indicator, without further considering depositional facies, palaeoclimate and tectonics (Morton and Hallsworth, 1999; Mange and Wright, 2007; von Eynatten and Dunkl, 2012).

The presence of prismatic zircon and tourmaline crystals throughout the successions of both study areas most likely indicates that some detritus was derived from fresh basement rocks. This would hint to a mixed recycled sedimentary and igneous provenance, under the assumption that the rounded zircon and tourmaline grains were derived from recycled sediments. Another explanation would be alluvial storage (Morton and Hallsworth, 1999) and/or constant reworking during deposition, accompanied by regular influxes of fresh material. In this scenario, the prismatic grains would represent the 'latest batch' of fresh detritus which consequently did not undergo much reworking before burial. A third possibility is input by an intermediate to felsic volcanic source (Morton et al., 1992).

The ZTR index of Devonian–Carboniferous samples decreases compared to Cambrian–Ordovician sandstones. Consequently, the latter units cannot have been the sole source for the late Palaeozoic successions. At least some input from freshly exposed basement is required to introduce the less stable heavy mineral phases. In this case, because of the specific stratigraphic context, the ZTR index does serve as a provenance indicator. The impoverished heavy mineral assemblage of the Cambrian–Ordovician sandstones is the result of extreme weathering coupled with low sedimentation rates (Avigad et al., 2005). Hirnantian samples from both study areas (Sarah, Zarqa and Sanamah formations) also exhibit very high ZTR values. Their depositional setting in a glacial context under cold conditions did allow for neither strong chemical weathering nor reworking during deposition. The high ZTR content must therefore largely be the result of sedimentary recycling, i.e., sourced from older sediments or sedimentary rocks. Similar values for the ATi from Hirnantian and Cambrian–Ordovician samples further support recycling over weathering. The slightly higher RZi values encountered in the Tabuk area hint to a somewhat higher contribution of metamorphic rocks compared to the Wajid area.

An increased contribution from metamorphic sources in the Devonian–Carboniferous Palaeozoic of southern Saudi Arabia is implied by the steady increase of the STi in the Wajid area from the Devonian onwards (Fig. 5). The RZi and STi patterns do not correlate in samples from the Tabuk area. While an increased RZi compared to Wajid samples indicates a higher metamorphic input, Tabuk samples are almost devoid of staurolite. Since the RZi is a more reliable provenance indicator, the absence of staurolite in the Tabuk area is probably either caused by dissolution or fractionation during transport.

Apatite is exceptionally resistant during burial diagenesis but highly susceptible to chemical weathering under surface conditions, especially in humid climates (Morton and Hallsworth, 2007). The comparatively low abundance of apatite and consequently low ATi encountered in most samples (Fig. 5) reinforces weathering and/or recycling rather than dissolution after burial as the main reason for their depleted heavy mineral assemblages. Knox et al. (2007) argued convincingly that ATi values are an original feature and not the result of Quaternary weathering. The very low ATi of lower Palaeozoic Tabuk samples compared to the corresponding Wajid succession is striking (Fig. 5). While this could be a genuine provenance signal pointing to a recycled sedimentary source, it is more likely the result of intensive weathering (Morton and Hallsworth, 1999). This begets the question as to why the Tabuk area experienced increased weathering during the early Palaeozoic compared to southern Saudi Arabia. Very localised climate differences or even different weather patterns seem improbable. Further transport and/or prolonged alluvial storage are better explanations. Yet these are by no means certain, since all concerned samples are quite proximal to their inferred source, the ANS. However, these observations would fit to a common, southerly provenance of the early Palaeozoic successions from both study areas. This would result in longer transport distances for central and northern Saudi Arabian sandstones. As discussed below, there arise problems with the rutile distribution in this model. Specifically the absence of high-grade rutile in the Dibsiyah Formation and significant differences in rutile source lithologies between the study areas do not support a common source. The detritus of the early Palaeozoic in both study areas was derived from distinct sources within the ANS, but the Saq and Qasim sediments experienced stronger weathering, probably caused by longer transport and/or alluvial storage. Hence, circumstances of different source areas and prolonged transport both are unclear so far. The high GZi in sample AB-SA98 is probably a real provenance signal, since it is accompanied by high RZi, ATi and STi (Fig. 5), which together indicate a large contribution from a nearby fresh metamorphic source and weak weathering conditions. This fits well with the glaciogenic depositional model of the Juwayl Formation (Keller et al., 2011).

The general composition of heavy mineral assemblages with a high ZTR fraction and few other meta- and unstable minerals is also observed in several other studies of the Palaeozoic of northern Gondwana (Powers et al., 1966; Hussain et al., 2004; Knox et al., 2007; Weissbrod and Bogoch, 2007; Morton et al., 2011; Garzanti et al., 2013). Yet in detail those studies differ significantly from each other and from this paper. Powers et al. (1966) observed mica (biotite and muscovite) in Palaeozoic sandstones from northern Saudi Arabia. Noteworthy mica content has not been reported from any of the other mentioned publications. The presence of biotite and muscovite in early and late Palaeozoic sandstones is surprising, since mica breaks down relatively easy during chemical weathering and mechanical abrasion. This is even more dubious as Powers et al. (1966) infer a recycled sedimentary provenance for the Palaeozoic sandstones. They also observed a remarkably impoverished heavy mineral assemblage for the Saq Formation compared to that of the Tawil Formation, which is in accordance with this study. Hussain et al. (2004) also observed high ZTR abundances with minor occurrences of hornblende, epidote and kyanite in samples from the southern Wajid area, which is contrasting to the results of this study. While some kyanite and epidote was observed in this study, they were much less abundant (Fig. 5). Hornblende was not present at all in the analysed samples. Hussain et al. (2004) interpreted this assemblage as derived from a mix of Neoproterozoic basement terranes and the 'Infracambrian' Ghabar Group in Yemen. They explicitly excluded the Arabian Shield as a significant source. It is noteworthy that they only studied the 125–250 µm grain-size fraction. Their results may therefore not necessarily be comparable to others since there is a grain-size dependence of heavy mineral composition (e.g., Garzanti et al., 2009; Krippner et al., 2015). The strong control of heavy mineral assemblages by hydraulic sorting related to grain size is well known (Garzanti et al., 2009). Krippner et al. (2015) demonstrated significant variances in the heavy mineral assemblages of different grain-size fractions from the same sample. They attributed grain size-dependant variability to different grain sizes of certain mineral phases in the host rocks and not to hydraulic sorting.

The compositional variations reported by Knox et al. (2007) in their study of Wajid Group sandstones have not been encountered to the same amount in the presented data set. Key differences are the lack of monazite and hornblende compared to the samples of Knox et al. (2007). Yet the general composition and compositional trend are similar to this study: a dominant ZTR fraction and a decrease of ultra-stable minerals towards younger strata. A drop of the RZi has been observed in this study as well, albeit not at the Sanamah–Dibsiyah boundary, but within the Dibsiyah Formation. This is mirrored to some degree in the Tabuk area. Although the RZi generally behaves twitchy, there is a significant drop between the Qasim and Sarah formations. Also similar to the data set of Knox et al. (2007) is the STi, which shows a significant increase in the Khusayyayn and Juwayl formations' strata compared to older samples from the Wajid area.

Weissbrod and Bogoch (2007) compiled heavy mineral data for, among others, Palaeozoic sandstones from the northern margin of the ANS (Fig. 8). The cited assemblages are again largely concordant with the results from Saudi Arabia. Cambrian–Ordovician sandstones from southern Israel and southern Jordan as well as Cambrian and Carboniferous sandstones from west central Sinai are dominated by ultra-stable heavy minerals and have consistently high ZTR values. Yet again differences appear in the accessory fractions of less stable minerals. Staurolite is reported from the Cambrian to Silurian from southern Jordan. In contrast, Tabuk samples are poor in staurolite (Fig. 3). The Late Ordovician and Silurian in southern Jordan also feature significant garnet. Likewise the abundance of apatite from the Cambrian of southern west central Sinai and southern Israel does not match Saudi Arabian assemblages. Weissbrod and Bogoch (2007) interpreted the heavy mineral assemblages of Cambrian–Ordovician sandstones as first-cycle detritus derived from the interior of Gondwana and transported over long distances, including extensive alluvial storage. In contrast, late Palaeozoic sandstones are thought to be mainly sourced from recycled, early Palaeozoic sediments. This interpretation does not fit completely with the data from Saudi Arabia. The reduction of ZTR values in later Palaeozoic units requires the input of at least some detritus derived from fresh basement outcrops, particularly regarding the greatly impoverished heavy mineral assemblages of lower Palaeozoic sandstones.

Knox et al. (2010) used SHMA to correlate sandstones of the Unayzah Formation in wells in central Saudi Arabia. They identified and characterised four heavy mineral units, largely corresponding to the established lithological subdivision of the Unayzah Formation reservoir. Furthermore, they recognised the influence of local sand influx and placer deposits and the problems associated with interpreting them. Unfortunately, they do not provide raw data, only chosen heavy mineral indices. Assigning a single surface sample from this study to one of the heavy mineral zones of Knox et al. (2010) is difficult: they rely heavily on trends to characterise the zones and employ indices not recorded in this study (monazite-zircon index, euhedral zircon index) and only studied subsurface samples. Furthermore, they did not consider staurolite and garnet or the corresponding indices (STi and GZi). Those minerals are heavily affected by burial dissolution and are absent in deeper parts of the wells. With these caveats in mind, sample AB-SA120 can tentatively assigned to the UNZ1B, because of low values for RZi and ATi and the absence of monazite (Fig. 5). According to this characterisation, the outcrop sample belongs to either the Unayzah A Member or the 'un-named middle Unayzah member'.

Compared with data from Palaeozoic sandstones of the eastern Murzuq Basin, Libya (Fig. 8), the presented data show general similarity, but differs in detail (Morton et al., 2011). The heavy mineral assemblage from the Murzuq Basin is largely impoverished, with a dominating ultra-stable fraction. Also similar is the occurrence of garnet in later Palaeozoic samples. Contrary to the observations from the Wajid and Tabuk areas is the continuously high ZTR in Devonian samples, indicating either a recycled sedimentary source or stronger weathering/longer transport than in Saudi Arabia. Morton et al. (2011) were also able to observe significant changes and trends in the RZi, which they used to identify distinct provenance events. These trends are not seen in the samples from the Tabuk and Wajid areas. Whether this is due to a generally more uniform provenance source or a result of lower sample density cannot be answered at this point. Furthermore, some of the Libyan

sandstones contain up to 7% monazite and some formations have abundant clinopyroxene. Both of those heavy minerals are nearly absent in this data set. The high GZi in the Silurian Tanezzuft Formation is another feature not recorded in Saudi Arabia.
Garzanti et al. (2013) published the heavy mineral assemblages of two samples from the early Palaeozoic of the Tabuk area: they consist almost entirely of the ZTR fraction plus anatase.

The very high amount of opaque phases is also reported by Hussain et al. (2004) as well as Weissbrod and Bogoch (2007). This indicates selective decomposition of meta- and unstable minerals (Hussain et al., 2004)

The high GZi of sample AB-SA98 (Fig. 5) raises the issue of placer deposits and sampling points. While most certainly a genuine provenance signal, the extremely high garnet content of the sample is curious, since such high garnet contents have not been reported by other workers. Furthermore, it is not replicated by the other two Juwayl samples and must be considered a placer deposit. Likewise while an increase in staurolite content and the STi was observed in this study, it did not reach the same scale as reported by Knox et al. (2007), although they sampled the same outcrop area. There seems to be a certain amount of bias involved during sampling. Consequently placer deposits can have a significant impact, especially if the overall sample density is low.

All cited studies confirmed the ultra-stable zircon, tourmaline and rutile as the main constituents of the heavy mineral assemblages of Palaeozoic sandstones from the northern Gondwana margin. Yet the variance in the accessory assemblages in those studies is surprising. Metastable and labile phases are especially affected, including garnet, staurolite, monazite, hornblende and epidote. There are several explanations for this variance: I) real regional and stratigraphic variance, i.e., provenance and weathering signals; II) sampling bias and placer deposits; III) differences in sample preparation and counting methods, i.e., systematic errors; IV) operator bias and/or misidentification. The latter one is especially troubling, since it is hard to estimate. SHMA with ‘manual’ mineral identification by different operators clearly has its limits, at the very least in the presented case.

4.2 Rutile varietal studies

The bulk of the rutile populations in both study areas are in the low- to medium-temperature range (Fig. 6). Potential sources for these rutiles are abundant in the nearby ANS and include medium-grade metamorphic and metasedimentary rocks as well as igneous rocks. The small population of high-T rutiles from the Saq Formation require a high-grade metamorphic source. Granulite-facies rocks are scarce in the ANS and are known only from small exposures in the eastern Afif Terrane of Saudi Arabia and the Barka Terrane in north-eastern Sudan (Johnson and Woldehaimanot, 2003) (Fig. 8). The nearest exposed granulitic rocks outside of the ANS are the granulite-facies gneisses of the Abas Gneiss Terrane and from Socotra Island, Yemen (Wahed et al., 2006; Denèle et al., 2012) (Fig. 8) as well as granulites from the Mozambique Belt and from south-eastern Sudan (Stern and Dawoud, 1991) (Fig. 8). A southerly provenance (in present-day orientation) of high-grade rutiles is problematic and seems unlikely: they were only found in the northern study area (Fig. 6). If the source area was to the south, the Dibsiyah Formation of the Wajid area would be expected to also contain a significant, if not larger, population. The fact that no high-T rutiles were found in the Wajid area makes the few exhumed granulite-facies rocks within the ANS the most likely source. Evidence that they were exposed in ancient times is given by the sub-Murdama unconformity in the eastern Afif Terrane. There, the late Proterozoic Murdama Group unconformably overlies granulites, which were extensively eroded (Johnson and Woldehaimanot, 2003). The presence of high-grade rutiles in the Saq Formation and their lack in the overlying Qasim Formation (Fig. 6) suggest a slight change in provenance. Such a change has also been observed by Hussain (2007). This was most likely a regional shift within the ANS rather than a large scale change in provenance. Progressive unroofing seems an unlikely cause for the change in rutile chemistry. This would result in an increase of high-grade rutiles in younger stratigraphic levels, which was not observed. The occurrence of very few (2) high-grade rutiles in the Devonian Jubah Formation (Fig. 6) hints at either a reactivation of the original granulitic source or at some degree of recycling of Saq sediments. Regional variance can also be seen in the source lithologies of detrital rutile assemblages. Rutiles from the Tabuk area have predominantly felsic source lithologies, while the Wajid area displays a larger mafic input (Fig. 6). Although mafic and ultra-mafic complexes are scarce in the Arabian Shield and constitute only 1% of its currently exposed surface area (Johnson et al., 2004), they are a potential sources for mafic rutiles. Examples are ultra-mafic complexes in the Midyan Terrane (Jackson et al., 1984) and mafic volcanic rocks from the Hali basin in the Asir Terrane (Johnson et al., 2013). Potential bimodal sources are present as well, for instance in the central Hijaz Terrane (Jackson et al., 1984) or in several volcanosedimentary basins (Murdama, Jibalah and Hibshi basins) in the Afif Terrane (Johnson et al., 2013). While this can only be considered a pilot study, varietal studies on detrital rutiles have shown to be a powerful tool in provenance studies of north Gondwanan Palaeozoic sandstones.

4.3 Garnet varietal studies

As Krippner et al. (2014) have recently shown, host rock identification using major element discrimination diagrams is feasible, but imprecise. According to these authors, the plot after Mange and Morton (2007), which is used in this study, has proven to contain significant overlap of different garnet host lithologies. This is partly because of the nature of the diagram, which uses solid lines as field boundaries and partly because of real overlap of specific garnet suites. Bearing that in mind, garnet discrimination diagrams can still prove useful when handled with care.

The distribution patterns of garnet host rock lithologies from both the Devonian Jubah Formation and the Carboniferous–Permian Juwayl Formation are remarkably similar (Fig. 7b, c), despite being separated both regionally and stratigraphically (Fig. 2). The main difference between the garnet populations of the two formations are the respective amounts of type

Ci (high-grade metamafic) and type Bii (amphibolite-facies metasedimentary) garnets. This is most probably not a genuine provenance signal. It must rather be attributed to the nature of the diagram and the fact that many garnets plot close to the discrimination line between the Ci and Bii fields (Fig. 7a). Considering this, the garnet populations of both formations are practically identical, indicating a common provenance. This is somewhat surprising given the distance between the outcrops and the distinctly different depositional environments of the two formations. The peri- and proglacial Juwayl Formation is expected to be more influenced by local garnet source, owing to a shorter transport distance and less opportunities for mixing and homogenisation of detritus. In contrast, the fluvial-deltaic to shallow marine Jubah Formation should display a more homogenised garnet population, covering a wider catchment area. A possible explanation is that the detritus of both formations is largely derived from an already homogenised sedimentary source. Yet sedimentary recycling is unlikely, since older units do not contain significant amounts of garnet. Dissolution of garnet in older formations is also not probable. Staurolite, which is like garnet unstable during deep burial, can still be found in some of the older Palaeozoic formations. Furthermore the outcrop area probably was never buried deeply enough to dissolve all garnet, given its position at the rim of the Arabian Shield. Therefore the most likely explanation for the similarity of the garnet populations from both formations is indeed a common provenance, dominated by detritus sourced in or proximal to the ANS.

The garnet distribution of Jauf Formation has to be evaluated carefully, since the sample population was extremely small, only containing 6 garnet grains. This sample size is unfortunately insufficient to compare with the other formations or to draw conclusions about provenance.

Potential source rocks for garnets are abundant in and around the ANS. Within the ANS they include garnet-sillimanite gneiss and granites from the southern Afif Terrain (Stacey and Agar, 1985; du Bray, 1988), garnet-biotite paraschists from the Kirsh gneiss dome (Al-Saleh, 2012) and granites from the Khida Terrane (du Bray, 1988, and own observations). Proximal to the

ANS lies the garnet-bearing Abas Gneiss Terrane in Yemen (Wahed et al., 2006) (Fig. 8). While sources for (felsic) igneous and metaigneous garnets are aplenty within the ANS and in its near vicinity, potential host rocks for metasedimentary and metamafic garnets are scarcer. Possible candidates are metapelites from the Central Eastern Desert in Egypt (Fritz et al., 2002), metavolcanics from the southern Red Sea Hills in Sudan (Kröner et al., 1991) and amphibolite-facies gneisses and metasediments from eastern and central Eritrea (Ghebreab, 1999; Woldehaimanot, 2001) (Fig. 8). Various metasedimentary and metaigneous rocks (including metabasites) from the Elat area in southern Israel (Cosca et al., 1999) (Fig. 8) could also serve as source, but are not in accordance with the northward sediment transport direction commonly inferred in the literature (Babalola, 1999; Hussain et al., 2000, 2004; Hussain, 2001; Wanas and Abdel-Maguid, 2006; Knox et al., 2007).

The presence of Type A garnets in all formations is interesting. They are most likely derived from granulite-facies metasedimentary rocks (Morton et al., 2004; Mange and Morton, 2007; Krippner et al., 2014). Yet such high-grade metasediments are rare in the ANS. They are known from the Barka Terrane in Eritrea, but no garnet has been reported from there (Johnson and Woldehaimanot, 2003). Significant sources for granulite-facies metasedimentary garnets are located more distally, in the Mozambique Belt and Sudan (Stern and Dawoud, 1991). While long-distance transport could explain the similar garnet distribution patterns of the Jubah and Juwayl formations, it is at odds with the glacigenic origin and sedimentological architecture of the latter, containing what are probably tunnel valleys (Keller et al., 2011). They imply shorter transport distances and suggest a proximal source within the ANS and/or Yemen. Other possible host lithologies for Type A garnets are intermediate to acidic deeper crust rocks and charnockites (Mange and Morton, 2007), yet these are also not prevalent within the ANS.

A potential proximal source for Type A garnets can be found in the Abas Gneiss Terrane in Yemen. This terrane contains garnet-bearing, granulite-facies paragneisses (Wahed et al., 2006). Although it is a potential candidate for granulite-facies detritus in the late Palaeozoic, it is unlikely to have supplied the high-T rutiles encountered in the Saq Formation of the Tabuk area. If the Abas Terrane was an active source during the early Palaeozoic, there should be at least some traces of high-grade minerals (granulite-facies garnet or rutile) in the Dibsiyah Formation of the Wajid area.

While a definite answer cannot be given at this point, a proximal source, probably to the south in Yemen, is the most likely cause for the presence of Type A garnets in the Jauf, Jubah and Juwayl formations, but did most likely not supply the granulite-facies rutiles of the Saq Formation.

5. Conclusions

1) The heavy mineral assemblages of Palaeozoic sediments from Saudi Arabia are typical for highly mature sandstones. Dominant phases are the ultra-stable fraction of zircon, tourmaline and rutile. Less stable accessories are apatite, garnet and staurolite. Input from a fresh basement source is indicated by the presence of some euhedral zircon and tourmaline throughout the succession.

2) The Hirnantian formations from both study areas were deposited in a glaciogenic context, but have very high ZTR values. They must therefore have been derived from mostly recycled sedimentary sources, since climatic and depositional conditions did not favour strong weathering.

3) While the principal heavy mineral composition of Saudi Arabian Palaeozoic sediments is similar to those from other parts of the northern Gondwana margin, they differ significantly in detail. Whether this is due to real variance or operator bias and misidentification could not be determined.

4) Rutile varietal studies reveal regional variance in rutile source lithologies: the Tabuk area contains predominantly felsic rutiles, while the Wajid area has a greater mafic input. The bulk of rutiles in both study areas were formed under low- to medium-temperature conditions. The Cambrian–Ordovician Saq Formation contains high-grade, granulite-facies rutiles, which are absent

in the overlying Qasim Formation and in the Wajid area. These high-grade rutiles from the Saq Formation were derived from a source north of the Wajid catchment. Rutile varietal studies have proven to be a powerful tool with great potential, yet more data from other units is needed.

5) Distribution patterns of garnet host rock lithologies from the Devonian Jubah and Carboniferous–Permian Juwayl formations are remarkably similar. They are both dominated by garnets derived from amphibolite-facies metasediments and intermediate to felsic igneous rocks. Both formations also contain garnets derived from granulite-facies metasediments. The nearest and most likely source are paragneisses in the Abas Gneiss Terrane, Yemen.

The Cambrian–Ordovician formations (Saq, Qasim, Dibsiyah) are first-cycle sediments, largely derived from the nearby Neoproterozoic basement of the ANS, but with varying transport distances. A minor, probably regional, provenance change from the Saq Formation to the Qasim Formation has been observed through rutile geochemistry. A second provenance change happened with the onset of the late Ordovician glaciation. The Hirnantian formations are not derived from the basement of the ANS but rather from recycled sedimentary sources, possibly the Cambrian-Ordovician sandstones. The third and last provenance change occurred either at the base of the Silurian or Devonian; late Palaeozoic units display an increasing input of fresh basement detritus. This can be linked to an increased tectonic segmentation of north-eastern Gondwana during conversion from a passive to an active continental margin in Devonian–Carboniferous time (Sharland et al., 2001).

Acknowledgements

This study has been enabled by the logistical support of the Gesellschaft für Internationale Zusammenarbeit (GIZ) and DornierConsulting (DCo) in Riyadh. We are indebted to Randolf Rausch and the staff of GIZ/DCo for their support during the 2013 field campaign. We further want to thank

Andreas Kronz for his help with EMP analyses. We thank Davide Lenaz and Jasper Knight for their constructive comments.

Appendix A. Supplementary data

Supplementary data associated with this article can be found, in the online version, at doi:xxxxxxxx

References

Al-Ajmi, H.F, Keller, M., Hinderer, M., Filomena, C.M., 2015. Lithofacies, depositional environments and stratigraphic architecture of the Wajid Group outcrops in southern Saudi Arabia. GeoArabia 20, 49–94.

Al-Harbi, O.A., Khan, M.M., 2005. Mineralogy and Geochemistry of Unayzah Formation, Central Saudi Arabia: Implications for Provenance Interpretation. Journal of King Saud University 18, 35–49.

Al-Harbi, O.A., Khan, M.M., 2008. Provenance, diagenesis, tectonic setting and geochemistry of Tawil Sandstone (Lower Devonian) in Central Saudi Arabia. Journal of Asian Earth Sciences 33, 278–287.

Al-Harbi, O.A., Khan, M.M., 2011. Source and origin of glacial paleovalley-fill sediments (Upper Ordovician) of Sarah Formation in central Saudi Arabia. Arabian Journal of Geosciences 4, 825–835.

Al-Laboun, A.A., 2010. Paleozoic tectono-stratigraphic framework of the Arabian Peninsula. Journal of King Saud University (Science) 22, 41–50.

Al-Saleh, A., 2012. The Kirsh gneiss dome: an extensional metamorphic core complex from the SE Arabian Shield. Arabian Journal of Geosciences 5, 335–344.

Alsharhan, A.S., 1994. Geology and hydrocarbon occurrences of the clastic Permo-Carboniferous in the central and eastern Arabian Basin. Geologie en Mijnbouw 73, 63–78.

Avigad, D., Kolodner, K., McWilliams, M., Persing, H., Weissbrod, T., 2003. Origin of northern Gondwana Cambrian sandstone revealed by detrital zircon SHRIMP dating. Geology 31, 227–230.

Avigad, D., Sandler. A., Kolodner, K., Stern, R.J., McWilliams, M., Miller, N., Beyth, M., 2005. Mass-production of Cambro-Ordovician quartz-rich sandstone as a consequence of chemical weathering of Pan-African terranes: Environmental implications. Earth and Planetary Sciences Letters 240, 818–826.

Babalola, L.O., 1999. Depositional Environments and Provenance of the Wajid Sandstone, Abha-Khamis Mushayt Area, Southwestern Saudi Arabia. MS Thesis, King Fahd University of Petroleum and Minerals, Dhahran, Saudi Arabia.

Cosca, M.A., Shimron, A., Caby, R., 1999. Late Precambrian metamorphism and cooling in the Arabian-Nubian Shield: Petrology and $^{40}Ar/^{39}Ar$ geochronology of metamorphic rocks of the Elat area (southern Israel). Precambrian Research 98, 107–127.

Denèle, Y., Leroy, S., Pelleter, E., Pik, R., Talbot, J.-Y., Khanbari, K., 2012. The Cryogenian arc formation and successive high-K calc-alkaline plutons of Socotra Island (Yemen). Arabian Journal of Geosciences 5, 903–924.

du Bray, E.A., 1988. Garnet compositions and their use as indicators of peraluminous granitoid petrogenesis – southeastern Arabian Shield. Contributions to Mineralogy and Petrology 100, 205–212.

Fritz, H., Dallmeyer, D.R., Wallbrecher, E., Loizenbauer, J., Hoinkes, G., Neumayr, P., Khudeir, A.A., 2002. Neoproterozoic tectonothermal evolution of the Central Eastern Desert, Egypt: a slow velocity tectonic process of core complex exhumation. Journal of African Earth Sciences 34, 137–155.

Garzanti, E., Andò, S., Vezzoli, G., 2008. Settling-equivalence of detrital minerals and grain-size dependence of sediment composition. Earth and Planetary Science Letters 273, 138–151.

Garzanti, E., Andò, S., Vezzoli, G., 2009. Grain-size dependence of sediment composition and environmental bias in provenance studies. Earth and Planetary Science Letters 277, 422–432.

Garzanti, E., Vermeesch, P., Andò, S., Vezzoli, G., Valagussa, M., Allen, K., Kadi, K.A., Al-Juboury, A.I.A., 2013. Provenance and recycling of Arabian desert sand. Earth-Science Reviews 120, 1–19.

Ghebreab, W., 1999. Tectono-metamorphic history of Neoproterozoic rocks in eastern Eritrea. Precambrian Research 98, 83–105.

Hubert, J.F., 1962. A zircon-tourmaline-rutile maturity index and the interdependence of the composition of heavy mineral assemblages with the gross composition and texture of sandstones. Journal of Sedimentary Research 32, 440–450.

Hussain, M., 2001. Framework mineralogy, diagenesis and provenance of the Wajid sandstone in Asir region, Southwestern Saudi Arabia. Unpublished report, KACST Project no. LPG 283.

Hussain, M., 2007. Elemental chemistry as a tool of stratigraphic correlation: A case study involving lower Paleozoic Wajid, Saq, and Qasim formations in Saudi Arabia. Marine and Petroleum Geology 24, 91–108.

Hussain, M., Babalola, L.O., Hariri, M.M., 2000. Provenance of the Wajid Sandstone, Southeastern Margin of the Arabian Shield: Geochemical and Petrographic Approach. American Association of Petroleum Geologists National Conference, New Orleans, USA, April 16, 1999, Extended Abstracts with Programs, pp. 7.

Hussain, M., Babalola, L.O., Hariri, M.M., 2004. Heavy minerals in the Wajid Sandstone from Abha-Khamis Mushayt area, southwestern Saudi Arabia: Implications on provenance and regional tectonic setting. GeoArabia 9, 77–102.

Hussain, M. Abdullatif, O.M., 2004. Trace Element Geochemistry and Heavy Mineral Assemblage of the Cambro-Ordovician Saq Sandstone of the Tabuk Basin and its Possible Correlation with the Wajid Sandstone of the Wajid Basin, Southwest Saudi Arabia. Final report, KACST Project LGP 6-54, 108 p.

Jackson, N.J., Walsh, J.N., Pegram, E., 1984. Geology, geochemistry and petrogenesis of late Precambrian granitoids in the Central Hijaz Region of the Arabian Shield. Contributions to Mineralogy and Petrology 87, 205–219.

Johnson, P.R., Woldehaimanot, B., 2003, Development of the Arabian-Nubian Shield: perspectives on accretion and deformation in the northern East African Orogen and the assembly of Gondwana. In: Yoshida, M., Windley, B.F., Dasgupta, S. (Eds.), Proterozoic East Gondwana: Supercontinent Assembly and Breakup. Geological Society, London, Special Publication 206, pp. 289–325.

Johnson, P.R., Kattan, F.H., Al-Saleh, A.M., 2004. Neoproterozoic ophiolites in the Arabian Shield: Field relations and structure. Developments in Precambrian Geology 13, 129–162.

Johnson, P.R., Halverson, G.P., Kusky, T.M., Stern, R.J., Pease, V., 2013. Volcanosedimentary Basins in the Arabian-Nubian Shield: Markers of Repeated Exhumation and Denudation in a Neoproterozoic Accretionary Orogen. Geosciences 3, 389–445.

Keller, M., Hinderer, M., Al-Ajmi, H.F., Rausch, R., 2011. Palaeozoic glacial depositional environments of SW Saudi Arabia: Process and product. In: Martini, I.P., French, H.M., Pérez Alberti, A. (Eds.), Icemarginal and periglacial processes and sediments. Geological Society, London, Special Publication 354, pp. 129–152.

Knox, R.W.O'B., Franks, S.G., Cocker, J.D., 2007. Stratigraphic evolution of heavy-mineral provenance signatures in the sandstones of the Wajid Group (Cambrian to Permian), southwestern Saudi Arabia. GeoArabia 12, 65–96.

Knox, R.W.O'B., Cocker, J.D., Filatoff, J., 2010. Heavy mineral stratigraphy of the Unayzah Formation and Basal Khuff Clastics (Carboniferous to Permian) of Central Saudi Arabia. GeoArabia 15, 17–80.

Kolodner, K., Avigad, D., McWilliams, M., Wooden, J.L., Weissbrod, T., Feinstein, S., 2006. Provenance of north Gondwana Cambrian-Ordovician sandstone: U-Pb SHRIMP dating of detrital zircons from Israel and Jordan. Geological Magazine 143, 367–391.

Konert, G., Al-Afifi, A.M., Al-Hajri, S.A., Droste, H.J., 2001. Paleozoic stratigraphy and hydrocarbon habitat of the Arabian Plate. GeoArabia 6, 407–442.

Krippner, A., Meinhold, G., Morton, A.C., von Eynatten, H., 2014. Evaluation of garnet discrimination diagrams using geochemical data of garnets derived from various host rocks. Sedimentary Geology 306, 36–52.

Krippner, A., Meinhold, G., Morton, A.C., Russell, E., von Eynatten, H., 2015. Grain-size dependence of garnet composition revealed by provenance signatures of modern stream sediments from the western Hohe Tauern (Austria). Sedimentary Geology, 321, 25–38.

Kröner, A., Linnebacher, P., Stern, R.J., Reischmann, T., Manton, W., Hussein, I.M., 1991. Evolution of Pan-African island arc assemblages in the southern Red Sea Hills, Sudan, and in southwestern Arabia as exemplified by geochemistry and geochronology. Precambrian Research 52, 99–118.

Linnemann, U., Ouzegane, K., Drareni, A., Hofmann, M., Becker, S., Gärtner, A., Sagawe, A., 2011. Sands of West Gondwana: An archive of secular magmatism and plate interactions—A case study from the Cambro-Ordovician section of the Tassili Ouan Ahaggar (Algerian Sahara) using U–Pb–LA-ICP-MS detrital zircon ages. Lithos 123, 188–203.

Lüning, S., Craig, J., Loydell, D.K., Štorch, P., Fitches, B., 2000. Lower Silurian 'hot shales' in North Africa and Arabia: regional distribution and depositional model. Earth-Science Reviews 49, 121–200.

Mange, M.A., Maurer, H.F.W., 1992. Heavy minerals in Colour. Chapman and Hall, London.

Mange, M.A. Morton, A.C., 2007. Geochemistry of heavy minerals. In: Mange, M.A., Wright, D.T. (Eds.), Heavy Minerals in Use. Developments in Sedimentology 58. Elsevier, Amsterdam, pp. 345–391.

Mange, M.A., Wright, D.T., 2007. Heavy Minerals in Use. Developments in Sedimentology 58. Elsevier, Amsterdam.

McGillivray, J.G., Husseini, M.I., 1992. The Paleozoic petroleum geology of Central Arabia. American Association of Petroleum Geologists Bulletin 76, 1473–1490.

Meinhold, G., 2010. Rutile and its applications in earth sciences. Earth-Science Reviews 102, 1–28.

Meinhold, G., Morton, A.C., Avigad, D., 2013. New insights into peri-Gondwana paleogeography and the Gondwana super-fan system from detrital zircon U–Pb ages. Gondwana Research 23, 661–665.

Meinhold, G., Anders, B., Kostopoulos, D., Reischmann, T., 2008. Rutile chemistry and thermometry as provenance indicator: An example from Chios Island, Greece. Sedimentary Geology 203, 98–111.

Meinhold, G., Morton, A.C., Fanning, C.M., Frei, D., Howard, J.P., Phillips, R.J., Strogen, D., Whitham, A.G., 2011. Evidence from detrital zircons for recycling of Mesoproterozoic and Neoproterozoic crust recorded in Paleozoic and Mesozoic sandstones of southern Libya. Earth and Planetary Science Letters 312, 164–175.

Melvin, J., 2015. Lithostratigraphy and depositional history of Upper Ordovician and lowermost Silurian sediments recovered from the Qusaiba-1 shallow core hole, Qasim region, central Saudi Arabia. Review of Palaeobotany and Palynology 212, 3–21.

Morag, N., Avigad, D., Gerdes, A., Belousova, E., Harlavan, Y., 2011. Detrital zircon Hf isotopic composition indicates long-distance transport of North Gondwana Cambrian–Ordovician sandstones. Geology 39, 955–958.

Morton, A.C., 1985. Heavy minerals in provenance studies. In: Zuffa, G.G. (Ed.), Provenance of Arenites. Riedel, Dortrecht, pp. 249–277.

Morton, A.C., Davies, J.R., Waters, R.A., 1992. Heavy minerals as a guide to turbidite provenance in the Lower Paleozoic southern Welsh basin: a pilot study. Geological Magazine 129, 573–580.

Morton, A.C. Hallsworth, C.R., 1994. Identifying provenance-specific features of detrital heavy mineral assemblages in sandstones. Sedimentary Geology 90, 241–256.

Morton, A.C. Hallsworth, C.R., 1999. Processes controlling the composition of heavy mineral assemblages in sandstones. Sedimentary Geology 124, 3–29.

Morton, A.C., Hallsworth, C., 2007. Stability of detrital heavy minerals during burial diagenesis. In: Mange, M.A., Wright, D.T. (Eds.), Heavy Minerals in Use. Developments in Sedimentology 58. Elsevier, Amsterdam, pp. 215–245.

Morton, A., Hallsworth, C., Chalton, B., 2004. Garnet compositions in Scottish and Norwegian basement terrains: a framework for interpretation of North Sea sandstone provenance. Marine and Petroleum Geology 21, 393–410.

Morton, A.C., Meinhold, G., Howard, J.P., Phillips, R.J., Strogen, D., Abutarruma, Y., Elgadry, M., Thusu, B., Whitham, A.G., 2011. A heavy mineral study of sandstones from the eastern Murzuq Basin, Libya: Constraints on provenance and stratigraphic correlation. Journal of African Earth Sciences 61, 308–330.

Pollastro, R.M., Karshbaum, A.S., Viger, R.J., 1998. Maps showing geology, oil and gas fields and geologic provinces of the Arabian Peninsula. United States Geological Survey, Open-File Report 97-470B, 14 p.

Powers, R.W., 1968. Lexique stratigraphique international. Volume III, Asie, Fas. 10 b1, Arabia Saoudite. Centre National de la Recherche Scientifique, Paris.

Powers, R.W., Ramirez, L.F., Redmond, C.D., Elberg, E.L. Jr., 1966. Geology of the Arabian Peninsula: Sedimentary geology of Saudi Arabia. United States Geological Survey Professional Paper 560-D, Washington.

Senalp. M., Al-Laboun, A.A., 2000. New evidence on the Late Ordovician glaciation in central Saudi Arabia. Saudi Aramco Journal of Technology, Spring 2000, 11–40.

Sharland, P.R., Archer, R., Casey, D.M., Davies, R.B., Hall, S.H., Heward, A.P., Horbury, A.D., Simmons, M.D., 2001. Arabian Plate sequence stratigraphy. GeoArabia Special Publication 2. Gulf PetroLink, Bahrain.

Stacey, J.S., Agar, R.A., 1985. U-Pb Isotopic evidence for the accretion of a continental microplate in the Zalm region of the Saudi Arabian Shield. Journal of the Geological Society 142, 1189–1203.

Stern, R.J., Dawoud, A.S., 1991. Late Precambrian (740 Ma) Charnockite, Enderbite, and Granite from Jebel Moya, Sudan: A Link between the Mozambique Belt and the Arabian-Nubian-Shield?. The Journal of Geology 99, 649–659.

Tomkins, H.S., Powell, R., Ellis, D.J., 2007. The pressure dependence of the zirconium-in-rutile thermometer. Journal of Metamorphic Geology 25, 703–713.

Triebold, S., von Eynatten, H., Luvizotto, G.L., Zack, T., 2007. Deducing source rock lithology from detrital rutile geochemistry: an example from the Erzgebirge, Germany. Chemical Geology 244, 421–436.

Triebold, S., von Eynatten, H., Zack, T., 2012. A recipe for the use of rutile in sedimentary provenance analysis. Sedimentary Geology 282, 268–275.

von Eynatten, H., Dunkl, I., 2012. Assessing the sediment factory: The role of single grain analysis. Earth-Science Reviews 115, 97–120.

Wahed, M.A., Zoheir, B., Hamimi, Z., Al-Selwi, K., 2006. Tectonic evolution of the Archaean-Neoproterozoic basement complex of Dhi Na'im-Al Bayda District, Republic of Yemen. Proceedings, 1st International Conference on Geology of the Arab World, Cairo University, Egypt.

Wanas, H.A., Abdel-Maguid, N.M., 2006. Petrography and geochemistry of the Cambro-Ordovician Wajid Sandstone, southwest Saudi Arabia: Implications for provenance and tectonic setting. Journal of Asian Earth Sciences 27, 416–429.

Watson, E.B., Wark, D.A., Thomas, J.B., 2006. Crystallisation thermometers for zircon and rutile. Contributions to Contributions to Mineralogy and Petrology 151, 413–433.

Weissbrod, T. and Bogoch, R., 2007. Distribution pattern and provenance implications of the heavy minerals in Neoproterozoic to Mesozoic siliciclastic successions in the Arabo-Nubian Shield and its northern periphery: a review. In: Mange, A.A., Wright, D.T. (Eds.), Heavy Minerals in Use, Developments in Sedimentology 58, Elsevier, Amsterdam, pp. 503–549.

Woldehaimanot, B., 2001. Extensional Tectonics in the High-Grade Metamorphic Terrain of Upper Anseba Region, Central Eritrea. Gondwana Research 4, 207–208.

Zack, T., von Eynatten, H., Kronz, A., 2004a. Rutile geochemistry and its potential use in quantitative provenance studies. Sedimentary Geology 171, 37–58.

Zack, T., Moraes, R., Kronz, A., 2004b. Temperature dependence of Zr in rutile: empirical calibration of a rutile thermometer. Contributions to Mineralogy and Petrology 148, 471–488.

FIGURE CAPTIONS

Fig. 1: Maps of the study areas. (a) Simplified geologic map of the Arabian Peninsula showing the study areas (modified after Powers, 1968). (b) Geologic map of the Wajid outcrop belt in southern Saudi Arabian, including sample points (modified after Keller et al., 2011). (c) Geologic map of the Tabuk area in northern Saudi Arabia, including sample points (modified after Pollastro et al., 1998).

Fig. 2: Simplified stratigraphic column of the Palaeozoic succession from southern (left) and central/northern (right) Saudi Arabia. Modified after 1) Al-Ajmi et al. (2015); 2) Al-Laboun (2010).

Fig. 3: Translucent heavy mineral distribution of Saudi Arabian Palaeozoic sandstones in their inferred stratigraphical order. Horizontal dashed lines mark formation boundaries. Dashed and dotted lines are correlative nonconformities related to the Hirnantian and Carboniferous–Permian glaciations. Formation thickness is not to scale. Dotted, grey areas represent the ultra-stable ZTR fraction. 'Other' fraction contains: monazite, kyanite, enstatite, epidote, tremolite, Cr-spinel, sphene and hornblende. See text for further explanation. (a) Tabuk area; (b) Wajid area.

Fig. 4: Photomicrographs of the most common heavy minerals. Black scale bars equal 50 µm. (a) Rounded zircon. (b) Euhedral zircons with fluid and mineral inclusions (upper row) and distinct zoning (bottom). (c) Rutile, upper right with distinct striation pattern. (d) Rounded and prismatic tourmaline,

some with fluid and mineral inclusions (bottom). (e) Apatite (upper row) and staurolite (bottom row). (f) Garnet with distinct etch markings.

Fig. 5: Different heavy mineral indices of samples from both study areas, plotted in their inferred stratigraphical succession. Formation thickness is not to scale. ZTR = zircon–tourmaline–rutile index; RZi = rutile–zircon index; GZi = garnet–zircon index; ATi = apatite–tourmaline index; STi = staurolite–tourmaline index; %Opq = percentage of opaque vs. translucent heavy minerals. See text for further explanation. (a) Tabuk area; (b) Wajid area.

Fig. 6: Frequency histograms of rutile temperature distribution from the Tabuk (a) and Wajid (b) areas. Bin width = 50 °C. (c) Data from (a) arrayed into formations. Temperatures have been calculated with the Zr-in-rutile thermometer after Tomkins et al. (2007), with P estimated at 10 kbar (see text for further explanation). Error bars are calculated for an error of T = 20 K. Note the distinct high-T population (≥800 °C; yellow box) in the Saq Formation of the Tabuk area. Inlays in (a) and (b) show the distribution of rutile source rock lithologies for lower and upper parts of the successions.

Fig. 7: Results of garnet chemical analysis. (a) Garnet classification scheme after Mange and Morton (2007). The corners of the ternary diagram represent one idealised garnet end members. Prp = pyrope, Alm = almandine, Sps = spessartine, Grs = grossular. A – sourced from granulite facies metasediments, charnockites or intermediate to acidic deeper crust rocks; Bi – from intermediate to acidic igneous rocks ; Bii – from amphibolite-facies metasediments; Ci – from high-grade metamafic rocks; Cii – from ultramafic rocks with high Mg; D – from Ca-rich metamorphites like metasomatic rocks (skarns), very low-grade metabasic rocks or ultra-high temperature calc-silicate granulites. Black symbols are values from garnet rims. (b), (c) and (d) Percentage distribution of garnet types in the Juwayl, Jubah and Jauf formations, respectively.

Fig. 8: Sketch map of the Arabian Peninsula and surrounding areas (modified after Powers, 1968; Avigad et al., 2005; Meinhold et al., 2013). White arrows show implicated sediment transport directions.

TABLE CAPTIONS

Table 1. Calculation and applications of heavy mineral indices used in this study (after Knox et al., 2011).

Index	Index minerals	Calculation	Application
ZTR	zircon, tourmaline, rutile	100 x Σ(zircon + tourmaline + rutile) / Σtranslucents	maturity
RZi	rutile, zircon	100 x rutile / (rutile + zircon)	provenance
GZi	garnet, zircon	100 x garnet / (garnet + zircon)	provenance
ATi	apatite, tourmaline	100 x apatite / (apatite + zircon)	maturity, provenance
STi	staurolite, tourmaline	100 x staurolite / (staurolite + tourmaline)	provenance

Table 2. Results of standard heavy mineral analysis in percent. Ratios of translucent phases were determined by counting 300 grains, when possible. The ratios of opaque to translucent phases were determined by counting 200 grains. Khus. = Khusayyayn, UT = upper Tabuk, LT = lower Tabuk, UW = upper Wajid, LW = lower Wajid, Zrc = zircon, Trm = tourmaline, Rtl = rutile, Apt = apatite, Grt = garnet, Stl = staurolite, Alt = alterated, Mzt = monazite, Ky = kyanite, En = enstatite, Epd = epidote, Trem = tremolite, Crs = Cr-spinel, Sph = sphene.

Sample	Stratigraphy	Zrc	Trm	Rtl	Apt	Grt	Stl	Alt	Mzt	Ky	En	Epd	Trem	Crs	Sph	Total
Tabuk area																
AB-SA120	Unayzah Fm.	59.67	16.33	5.33	1.33	3.67	12.00	1.67	0.00	0.00	0.00	0.00	0.00	0.00	0.00	300
AB-SA150	Jubah Fm.	31.67	37.00	8.67	4.33	7.67	0.00	5.67	0.00	0.00	5.00	0.00	0.00	0.00	0.00	300
AB-SA152	Jubah Fm.	60.33	16.33	10.33	4.33	4.33	3.33	1.00	0.00	0.00	0.00	0.00	0.00	0.00	0.00	300
AB-SA153	Jubah Fm.	29.00	33.33	4.67	0.67	17.00	0.00	9.00	0.67	0.00	3.33	2.33	0.00	0.00	0.00	300
AB-SA160/T	Jauf Fm.	45.67	42.67	11.33	0.00	0.00	0.00	0.00	0.33	0.00	0.00	0.00	0.00	0.00	0.00	300
AB-SA161	Jauf Fm.	51.33	31.67	9.33	4.67	0.00	0.00	2.67	0.33	0.00	0.00	0.00	0.00	0.00	0.00	300
AB-SA164	Jauf Fm.	50.67	19.00	13.00	1.67	14.67	0.00	1.00	0.00	0.00	0.00	0.00	0.00	0.00	0.00	300
AB-SA156	Tawil Fm.	56.00	24.67	7.33	1.33	4.33	0.00	5.00	1.33	0.00	0.00	0.00	0.00	0.00	0.00	300
AB-SA157	Tawil Fm.	46.00	42.33	9.33	0.33	0.00	0.00	0.67	1.33	0.00	0.00	0.00	0.00	0.00	0.00	300
AB-SA128	Sharawra Mbr.	7.33	24.00	2.33	4.33	0.33	0.00	61.00	0.67	0.00	0.00	0.00	0.00	0.00	0.00	300
AB-SA127	Sharawra Mbr.	51.96	28.47	13.52	3.56	1.07	0.00	0.00	1.42	0.00	0.00	0.00	0.00	0.00	0.00	281
AB-SA132/2	Zarqa Fm.	42.33	33.67	19.67	0.33	0.00	0.00	2.33	1.67	0.00	0.00	0.00	0.00	0.00	0.00	300
AB-SA132/1	Zarqa Fm.	53.44	22.75	14.29	5.29	4.23	0.00	0.00	0.00	0.00	0.00	0.00	0.00	0.00	0.00	189
AB-SA123/2	Sarah Fm.	82.33	12.33	4.33	0.00	0.00	0.67	0.00	0.33	0.00	0.00	0.00	0.00	0.00	0.00	300
AB-SA122/2	Sarah Fm.	62.00	25.00	8.00	0.00	0.00	1.00	1.00	1.00	0.00	0.00	0.00	0.00	0.00	2.00	300
AB-SA124	Qasim Fm.	24.33	59.00	15.33	0.67	0.00	0.00	0.00	0.67	0.00	0.00	0.00	0.00	0.00	0.00	300
AB-SA126	Qasim Fm.	23.33	63.00	11.33	0.33	0.00	0.00	1.33	0.67	0.00	0.00	0.00	0.00	0.00	0.00	300
AB-SA145	Qasim Fm.	51.33	36.00	9.00	1.00	0.00	0.00	2.00	0.67	0.00	0.00	0.00	0.00	0.00	0.00	300
AB-SA142/2	Qasim Fm.	48.00	30.33	16.00	0.00	0.00	0.00	4.00	1.67	0.00	0.00	0.00	0.00	0.00	0.00	300
AB-SA144/1	Qasim Fm.	51.67	42.33	5.67	0.33	0.00	0.00	0.00	0.00	0.00	0.00	0.00	0.00	0.00	0.00	300
AB-SA170	Saq Fm.	37.33	48.00	14.67	0.00	0.00	0.00	0.00	0.00	0.00	0.00	0.00	0.00	0.00	0.00	300
AB-SA167	Saq Fm.	42.33	38.00	9.33	0.00	0.00	5.00	5.33	0.00	0.00	0.00	0.00	0.00	0.00	0.00	300

AB-SA169	Saq Fm.	51.00	39.67	5.00	0.00	0.00	0.00	3.33	1.00	0.00	0.00	0.00	0.00	0.00	0.00	300
Wajid area																
AB-SA98	Juwayl Fm.	5.33	4.33	3.00	10.00	53.67	6.33	16.00	0.00	0.33	0.33	0.00	0.00	0.67	0.00	300
AB-SA80	Juwayl Fm.	55.00	19.33	4.00	4.00	0.33	11.67	1.00	0.00	4.00	0.67	0.00	0.00	0.00	0.00	300
AB-SA100	Juwayl Fm.	53.67	26.67	4.33	0.00	0.67	13.00	0.00	0.00	0.00	1.33	0.00	0.00	0.33	0.00	300
AB-SA87	Khusayyayn Fm.	59.29	17.70	6.19	2.65	1.77	6.19	0.88	0.00	3.54	0.00	0.00	0.00	1.77	0.00	113
AB-SA89	Khusayyayn Fm.	37.33	35.00	6.67	2.33	0.33	15.00	1.67	0.00	1.00	0.00	0.00	0.00	0.67	0.00	300
AB-SA90	Khusayyayn Fm.	27.87	42.62	4.10	8.20	0.00	6.56	4.92	0.00	0.00	0.82	0.00	4.92	0.00	0.00	122
AB-SA118	Khusayyayn Fm.	40.93	42.35	3.56	1.07	0.00	7.83	3.20	0.00	0.00	0.71	0.36	0.00	0.00	0.00	281
AB-SA32	Khusayyayn Fm.	11.67	32.50	10.00	25.83	0.83	5.00	12.50	0.00	0.83	0.00	0.83	0.00	0.00	0.00	120
AB-SA115	Qusaiba Mbr.	7.33	8.33	0.33	17.00	1.00	0.00	66.00	0.00	0.00	0.00	0.00	0.00	0.00	0.00	300
AB-SA62	Sanamah Fm.	69.67	14.67	8.00	5.33	0.00	0.00	0.00	2.00	0.00	0.00	0.00	0.00	0.00	0.00	300
AB-SA63	Sanamah Fm.	56.67	29.00	5.33	4.00	0.00	4.33	0.67	0.00	0.00	0.00	0.00	0.00	0.00	0.00	300
AB-SA64	Sanamah Fm.	60.67	22.33	11.00	1.00	0.33	0.00	3.33	1.33	0.00	0.00	0.00	0.00	0.00	0.00	300
AB-SA74	Dibsiyah Fm.	81.00	9.33	8.67	0.67	0.33	0.00	0.00	0.00	0.00	0.00	0.00	0.00	0.00	0.00	300
AB-SA76	Dibsiyah Fm.	62.67	24.00	7.00	3.67	0.00	2.00	0.33	0.00	0.00	0.00	0.00	0.00	0.33	0.00	300
AB-SA72	Dibsiyah Fm.	35.67	42.00	13.67	0.67	0.00	0.33	6.67	1.00	0.00	0.00	0.00	0.00	0.00	0.00	300
AB-SA69	Dibsiyah Fm.	56.07	24.30	14.49	1.87	0.00	0.00	2.80	0.47	0.00	0.00	0.00	0.00	0.00	0.00	214
AB-SA79	Dibsiyah Fm.	63.67	26.33	7.67	1.00	0.00	0.67	0.33	0.00	0.00	0.00	0.00	0.00	0.33	0.00	300

Table 3. Results of standard heavy mineral analysis in percent expressed in heavy mineral indices. Opq% = percentage of opaque phases, ZTR = zircon–tourmaline–rutile index, RZi = rutile–zircon index, MZi = monazite–zircon index, GZi = garnet–zircon index, ATi = apatite–tourmaline index, HTi = hornblende–tourmaline index, STi = staurolite–tourmaline index.

Sample	Stratigraphy	Opq%	ZTR	RZi	MZi	GZi	ATi	HTi	STi
Tabuk area									
AB-SA120	Unayzah Fm.	86.50	81.33	8.21	0.00	5.79	7.55	0.00	42.35
AB-SA150	Jubah Fm.	75.50	77.33	21.49	0.00	19.49	10.48	0.00	0.00
AB-SA152	Jubah Fm.	67.00	87.00	14.62	0.00	6.70	20.97	0.00	16.95
AB-SA153	Jubah Fm.	90.00	67.00	13.86	2.25	36.96	1.96	0.00	0.00
AB-SA160/T	Jauf Fm.	56.00	99.67	19.88	0.72	0.00	0.00	0.00	0.00
AB-SA161	Jauf Fm.	86.50	92.33	15.38	0.65	0.00	12.84	0.00	0.00
AB-SA164	Jauf Fm.	47.00	82.67	20.42	0.00	22.45	8.06	0.00	0.00
AB-SA156	Tawil Fm.	62.00	88.00	11.58	2.33	7.18	5.13	0.00	0.00
AB-SA157	Tawil Fm.	42.00	97.67	16.87	2.82	0.00	0.78	0.00	0.00
AB-SA128	Sharawra Mbr.	65.00	33.67	24.14	8.33	4.35	15.29	0.00	0.00
AB-SA127	Sharawra Mbr.	80.00	93.95	20.65	2.67	2.01	11.11	0.00	0.00
AB-SA132/2	Zarqa Fm.	32.00	95.67	31.72	3.79	0.00	0.98	0.00	0.00
AB-SA132/1	Zarqa Fm.	97.50	90.48	21.09	0.00	7.34	18.87	0.00	0.00
AB-SA123/2	Sarah Fm.	53.00	99.00	5.00	0.40	0.00	0.00	0.00	5.13
AB-SA122/2	Sarah Fm.	49.00	95.00	11.43	1.59	0.00	0.00	0.00	3.85
AB-SA124	Qasim Fm.	25.00	98.67	38.66	2.67	0.00	1.12	0.00	0.00
AB-SA126	Qasim Fm.	44.50	97.67	32.69	2.78	0.00	0.53	0.00	0.00
AB-SA145	Qasim Fm.	90.50	96.33	14.92	1.28	0.00	2.70	0.00	0.00
AB-SA142/2	Qasim Fm.	58.50	94.33	25.00	3.36	0.00	0.00	0.00	0.00
AB-SA144/1	Qasim Fm.	73.50	99.67	9.88	0.00	0.00	0.78	0.00	0.00
AB-SA170	Saq Fm.	44.00	100.00	28.21	0.00	0.00	0.00	0.00	0.00
AB-SA167	Saq Fm.	54.50	89.67	18.06	0.00	0.00	0.00	0.00	11.63
AB-SA169	Saq Fm.	81.00	95.67	8.93	1.92	0.00	0.00	0.00	0.00
Wajid area									

AB-SA98	Juwayl Fm.	78.00	12.67	36.00	0.00	90.96	69.77	0.00	59.38
AB-SA80	Juwayl Fm.	70.00	78.33	6.78	0.00	0.60	17.14	0.00	37.63
AB-SA100	Juwayl Fm.	41.50	84.67	7.47	0.00	1.23	0.00	0.00	32.77
AB-SA87	Khusayyayn Fm.	75.00	83.19	9.46	0.00	2.90	13.04	0.00	25.93
AB-SA89	Khusayyayn Fm.	75.00	79.00	15.15	0.00	0.88	6.25	0.00	30.00
AB-SA90	Khusayyayn Fm.	97.00	74.59	12.82	0.00	0.00	16.13	0.00	13.33
AB-SA118	Khusayyayn Fm.	80.00	86.83	8.00	0.00	0.00	2.46	0.00	15.60
AB-SA32	Khusayyayn Fm.	92.00	54.17	46.15	0.00	6.67	44.29	0.00	13.33
AB-SA115	Qusaiba Mbr.	96.00	16.00	4.35	0.00	12.00	67.11	0.00	0.00
AB-SA62	Sanamah Fm.	71.50	92.33	10.30	2.79	0.00	26.67	2.22	0.00
AB-SA63	Sanamah Fm.	48.50	91.00	8.60	0.00	0.00	12.12	0.00	13.00
AB-SA64	Sanamah Fm.	53.00	94.00	15.35	2.15	0.55	4.29	0.00	0.00
AB-SA74	Dibsiyah Fm.	64.50	99.00	9.67	0.00	0.41	6.67	0.00	0.00
AB-SA76	Dibsiyah Fm.	56.00	93.67	10.05	0.00	0.00	13.25	0.00	7.69
AB-SA72	Dibsiyah Fm.	57.50	91.33	27.70	2.73	0.00	1.56	0.00	0.79
AB-SA69	Dibsiyah Fm.	71.50	94.86	20.53	0.83	0.00	7.14	0.00	0.00
AB-SA79	Dibsiyah Fm.	79.00	97.67	10.75	0.00	0.00	3.66	0.00	2.47

Table 4. Number of mafic and felsic rutiles in both study areas.

Formation	Study area	mafic	felsic	total
Jubah	Upper Tabuk	8	45	53
Qasim	Lower Tabuk	8	22	30
Saq	Lower Tabuk	12	31	43
Juwayl	Upper Wajid	9	4	13
Sanamah	Lower Wajid	12	16	28
Dibsiyah	Lower Wajid	16	16	32

Figure 1

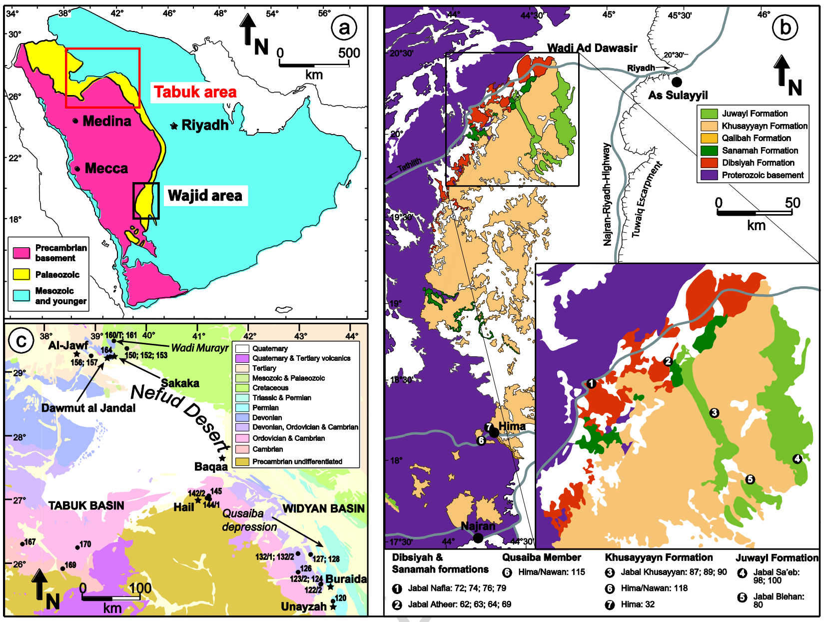
a
Tabuk area
Medina
Riyadh
Mecca
Wajid area
Precambrian basement
Palaeozoic
Mesozoic and younger
0 500 km
N
b
Wadi Ad Dawasir
Riyadh
As Sulayyil
Juwayl Formation
Khusayyayn Formation
Qalibah Formation
Sanamah Formation
Dibsiyah Formation
Proterozoic basement
0 50 km
Najran-Riyadh-Highway
Tuwaiq Escarpment
Hima
Najran
Dibsiyah & Sanamah formations
1 Jabal Nafla: 72; 74; 76; 79
2 Jabal Atheer: 62; 63; 64; 69
Qusaiba Member
6 Hima/Nawan: 115
Khusayyayn Formation
3 Jabal Khusayyan: 87; 89; 90
6 Hima/Nawan: 118
7 Hima: 32
Juwayl Formation
4 Jabal Sa'eb: 98; 100
5 Jabal Blehan: 80
c
Al-Jawf
Wadi Murayr
Sakaka
Dawmut al Jandal
Nefud Desert
Baqaa
TABUK BASIN
Hail
WIDYAN BASIN
Qusaiba depression
Buraida
Unayzah
0 100 km
Quaternary
Quaternary & Tertiary volcanics
Tertiary
Mesozoic & Palaeozoic
Cretaceous
Triassic & Permian
Permian
Devonian
Devonian, Ordovician & Cambrian
Ordovician & Cambrian
Cambrian
Precambrian undifferentiated

Figure 2

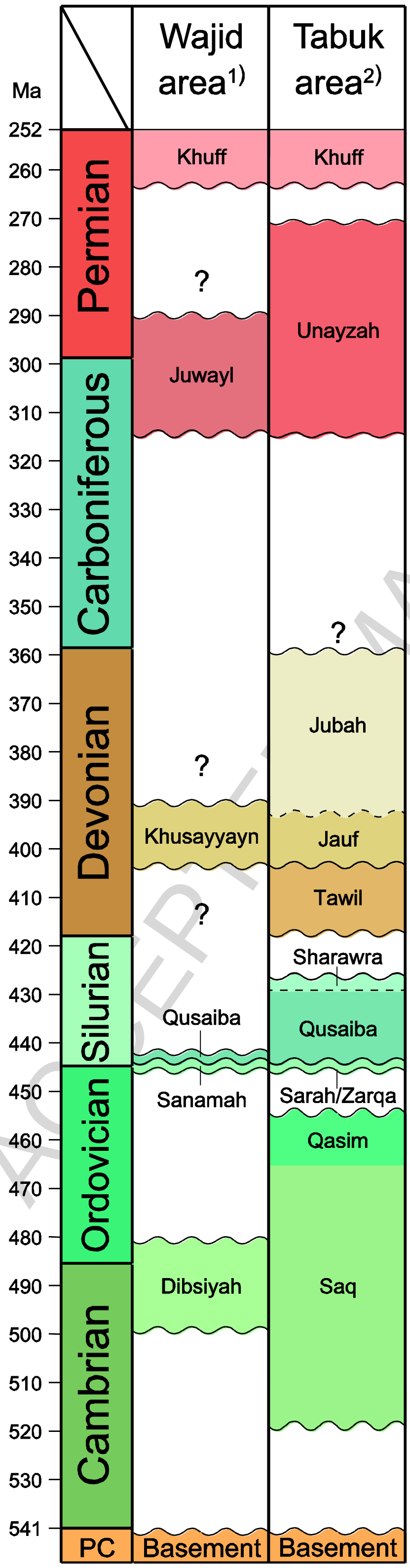

Wajid area1)
Tabuk area2)
Ma
252
260
270
280
290
300
310
320
330
340
350
360
370
380
390
400
410
420
430
440
450
460
470
480
490
500
510
520
530
541
Permian
Carboniferous
Devonian
Silurian
Ordovician
Cambrian
PC
Khuff
Khuff
?
Unayzah
Juwayl
?
Jubah
?
Khusayyayn
Jauf
?
Tawil
Sharawra
Qusaiba
Qusaiba
Sanamah
Sarah/Zarqa
Qasim
Dibsiyah
Saq
Basement
Basement

Figure 3

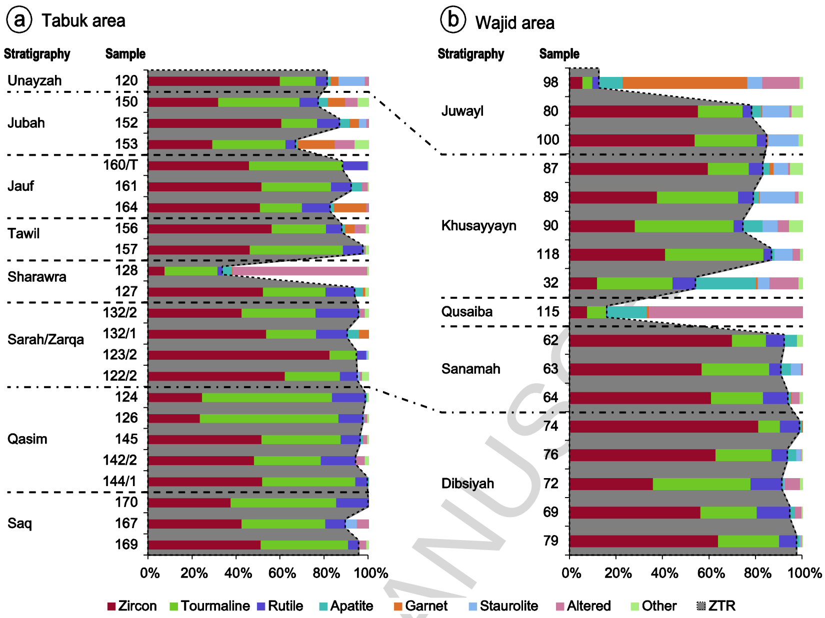

a Tabuk area
b Wajid area
Stratigraphy
Sample
Unayzah
Jubah
Jauf
Tawil
Sharawra
Sarah/Zarqa
Qasim
Saq
120
150
152
153
160/T
161
164
156
157
128
127
132/2
132/1
123/2
122/2
124
126
145
142/2
144/1
170
167
169
Juwayl
Khusayyayn
Qusaiba
Sanamah
Dibsiyah
98
80
100
87
89
90
118
32
115
62
63
64
74
76
72
69
79
0%
20%
40%
60%
80%
100%
Zircon
Tourmaline
Rutile
Apatite
Garnet
Staurolite
Altered
Other
ZTR

Figure 4

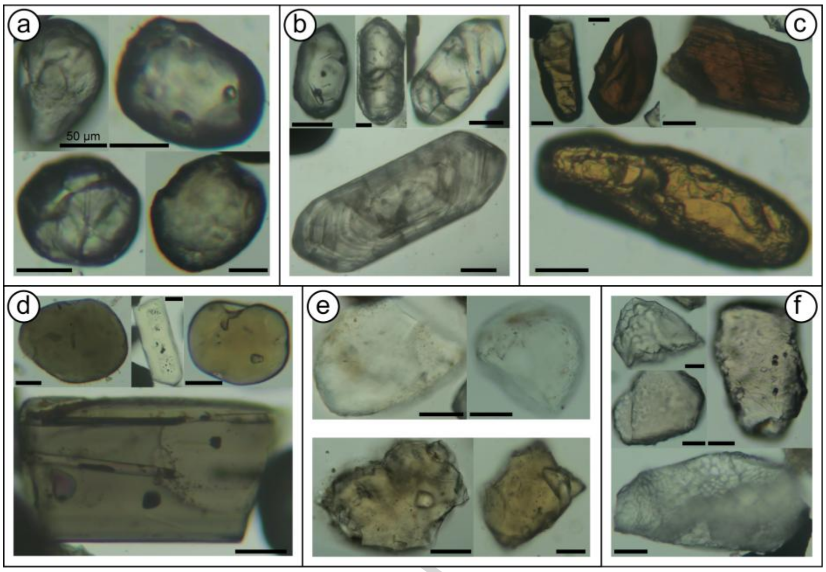

Figure 5

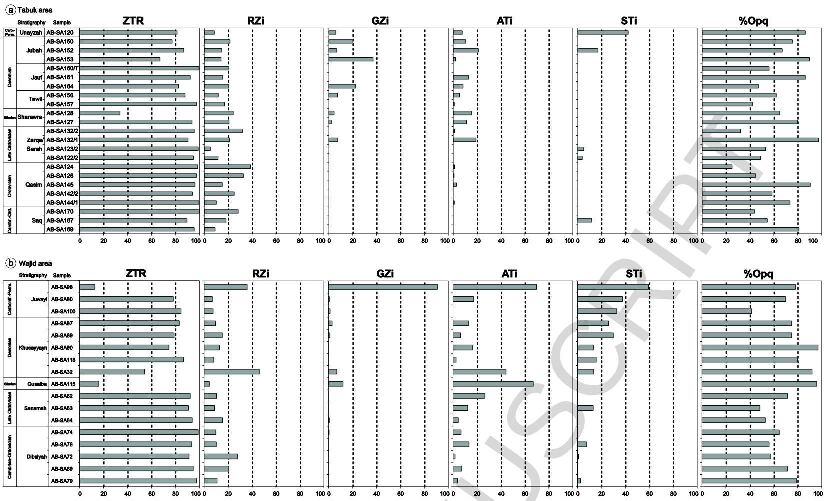

a Tabuk area
Stratigraphy
Sample
ZTR
RZi
GZi
ATI
STI
%Opq
Carb.-Perm.
Unayzah
AB-SA120
Devonian
Jubah
AB-SA150
AB-SA152
AB-SA153
Jauf
AB-SA160/T
AB-SA161
AB-SA164
Tawil
AB-SA156
AB-SA157
Silurian
Sharawra
AB-SA128
AB-SA127
Late Ordovician
Zarqa/Sarah
AB-SA132/2
AB-SA132/1
AB-SA123/2
AB-SA122/2
Ordovician
Qasim
AB-SA124
AB-SA126
AB-SA145
AB-SA142/2
AB-SA144/1
Cambr.-Ord.
Saq
AB-SA170
AB-SA167
AB-SA169
0 20 40 60 80 100
b Wajid area
Stratigraphy
Sample
ZTR
RZi
GZi
ATI
STI
%Opq
Carbonif.-Perm.
Juwayl
AB-SA98
AB-SA80
AB-SA100
Devonian
Khusayyayn
AB-SA87
AB-SA89
AB-SA90
AB-SA118
AB-SA32
Silurian
Qusaiba
AB-SA115
Late Ordovician
Sanamah
AB-SA62
AB-SA63
AB-SA64
Cambrian-Ordovician
Dibsiyah
AB-SA74
AB-SA76
AB-SA72
AB-SA69
AB-SA79
0 20 40 60 80 100

Figure 6

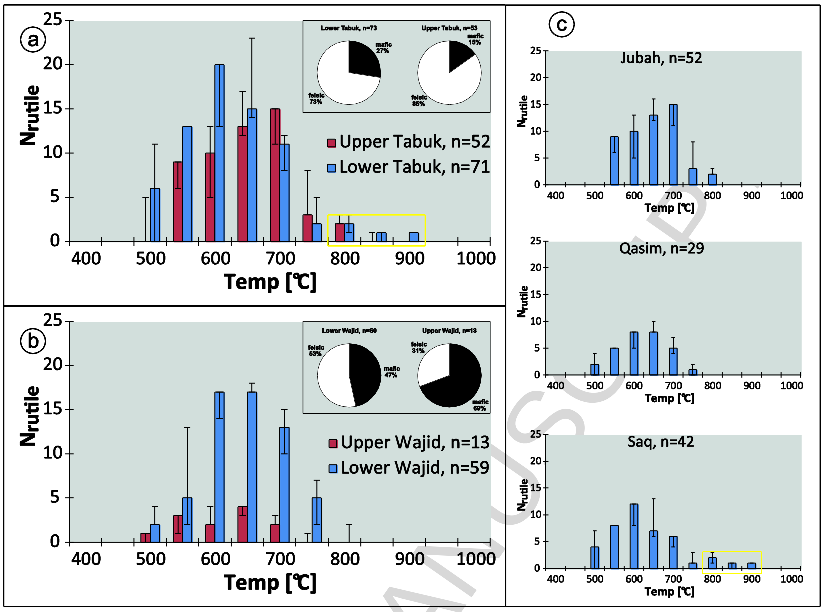
a
b
c
Nrutile
Temp [℃]
Lower Tabuk, n=73
Upper Tabuk, n=53
mafic 27%
felsic 73%
mafic 15%
felsic 85%
Upper Tabuk, n=52
Lower Tabuk, n=71
Lower Wajid, n=60
Upper Wajid, n=13
felsic 53%
mafic 47%
felsic 31%
mafic 69%
Upper Wajid, n=13
Lower Wajid, n=59
Jubah, n=52
Qasim, n=29
Saq, n=42

Figure 7

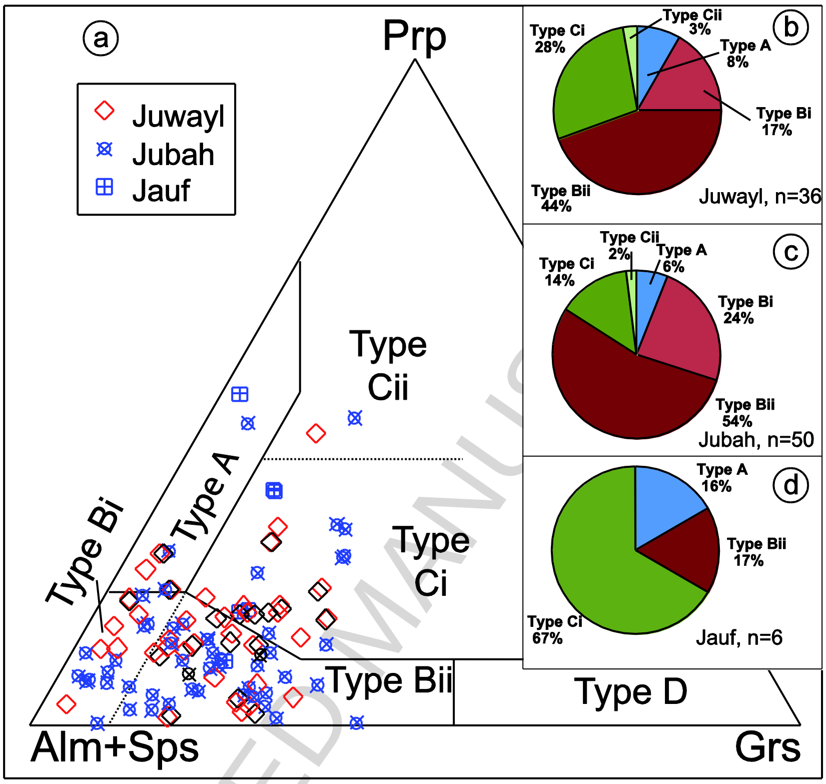
a
Prp
Juwayl
Jubah
Jauf
Type Cii
Type A
Type Bi
Type Ci
Type Bii
Type D
Alm+Sps
Grs
b
Type Cii 3%
Type Ci 28%
Type A 8%
Type Bi 17%
Type Bii 44%
Juwayl, n=36
c
Type Cii 2%
Type A 6%
Type Ci 14%
Type Bi 24%
Type Bii 54%
Jubah, n=50
d
Type A 16%
Type Bii 17%
Type Ci 67%
Jauf, n=6

Figure 8

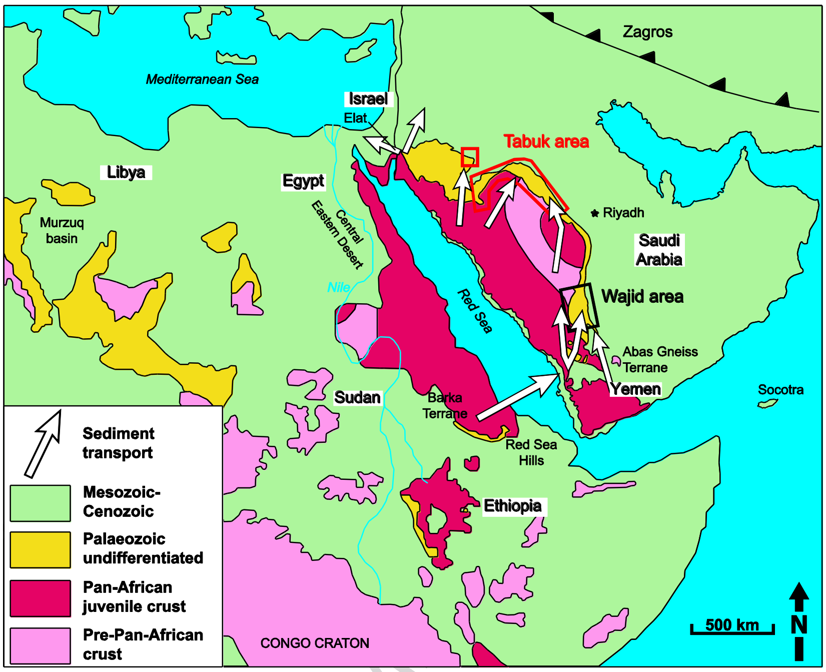
Zagros
Mediterranean Sea
Israel
Elat
Tabuk area
Libya
Egypt
Riyadh
Murzuq basin
Central Eastern Desert
Saudi Arabia
Nile
Red Sea
Wajid area
Abas Gneiss Terrane
Yemen
Socotra
Sudan
Barka Terrane
Red Sea Hills
Ethiopia
Sediment transport
Mesozoic-Cenozoic
Palaeozoic undifferentiated
Pan-African juvenile crust
Pre-Pan-African crust
CONGO CRATON
500 km
N